2015-07-01

Histone Deacetylase 6 (HDAC6) Is Critical for Tumor Cell Survival and Promotes the Pro-Survival Activity of 14-3-3ζ viaDeacetylation of Lysines Within the14-3-3ζ Binding Pocket

Jeffrey Benjamin Mortenson
Brigham Young University - Provo

Histone Deacetylase 6 (HDAC6) Is Critical for Tumor Cell Survival and Promotes the Pro-Survival Activity of 14-3-3ζ via Deacetylation of Lysines Within the 14-3-3ζ Binding Pocket

Jeffrey Benjamin Mortenson

A thesis submitted to the faculty of
Brigham Young University
in partial fulfillment of the requirements for the degree of

Master of Science

Joshua L. Andersen, Chair
Barry M. Willardson
David M. Thomson

Department of Chemistry and Biochemistry

Brigham Young University

July 2015

ABSTRACT

Histone Deacetylase 6 (HDAC6) Is Critical for Tumor Cell Survival
and Promotes the Pro-Survival Activity of 14-3-3ζ via
Deacetylation of Lysines Within the
14-3-3ζ Binding Pocket

Jeffrey Benjamin Mortenson
Department of Chemistry and Biochemistry, BYU
Master of Science

Our understanding of non-histone acetylation as a means of cellular regulation is in its infancy. Using a mass spectrometry approach we identified acetylated lysine residues and monitored acetylation changes across the proteome as a consequence of metabolic stress (hypoxia). We observed changes in acetylation status of non-histone lysines in tumor cells. Through the use of small molecule inhibitors of histone deacetylase enzymes (HDACs) and siRNA screening identified HDAC6 as a pro-survival regulator of lysine acetylation during hypoxia.

The phospho-binding protein 14-3-3ζ acts as a signaling hub controlling a network of interacting partners and oncogenic pathways. We show here that lysines within the 14-3-3ζ binding pocket and protein-protein interface can be modified by acetylation. The positive charge on two of these lysines, K49 and K120, is critical for coordinating 14-3-3ζ-phosphoprotein interactions. Through screening, we identified HDAC6 as the K49/K120 deacetylase. Inhibition of HDAC6 blocks 14-3-3ζ interactions with two well-described interacting partners, Bad and AS160, which triggers their dephosphorylation at S112 and T642, respectively. Expression of an acetylation-refractory K49R/K120R mutant of 14-3-3ζ rescues both the HDAC6 inhibitor-induced loss of interaction and S112/T642 phosphorylation. Furthermore, expression of the K49R/K120R mutant of 14-3-3ζ inhibits the cytotoxicity of HDAC6 inhibition. These data demonstrate a novel role for HDAC6 in controlling 14-3-3ζ binding activity.

Keywords: Non-histone acetylation, cell survival, 14-3-3, HDAC6

ACKNOWLEDGEMENTS

This work was supported by funding from the Elsa U. Pardee Foundation and a Simmons Center for Cancer Research Award to the Andersen lab. We thank members of the Kornbluth (Duke University) and Andersen laboratories for their assistance and thoughtful discussions. We thank members of the Willardson laboratory (BYU) for generously sharing reagents.

TABLE OF CONTENTS

LIST OF TABLES

LIST OF FIGURES

CHAPTER 1: INTRODUCTION

The health of the overall organism depends on the ability of each individual cell to carry out its necessary functions. For a cell to function properly in this context, it must sense environment cues and communicate these to gene expression machinery within the nucleus via cell signaling pathways. As such, cellular pathways are tightly regulated to ensure proper functionality within the scope of the good of the entire organism. The deregulation of cellular pathways can have serious consequences to the organism including the development of cancer and degenerative diseases. These cell signaling pathways are controlled in large part by the addition (and removal) of post-translational modifications (PTMs) to proteins within the pathway. The best studied PTM is the addition and removal of phosphate groups to serine, threonine, and tyrosine residues. Other modifications have gained interest in more recent years due to our understanding of their scope and importance to cellular regulation. My thesis focuses on understanding a relatively poorly understood PTM, lysine acetylation, and its impact on the function of the critical cell signaling regulator 14-3-3ζ.

Lysine residues are subjected to a variety of PTMs. The dynamic addition and removal of methyl groups, ubiquitin groups, poly-ubiquitin groups, glycosyl groups, and lipid groups are under investigation for their role in modulating the function of the protein they decorate (1,2,3). Acetylation, another lysine modification, has received increasing attention recently for its role in protein regulation. The addition of an acetyl group on the free ε-amino group of lysine residues is carried out by cellular enzymes known as histone acetyltransferases (HATs). HATs are ubiquitously expressed in all higher order eukaryotes and have long been known to catalyze the addition of acetyl groups to free lysine residues of histone proteins, thus the name (4). Free amino groups on lysine side chains hold a positive electrostatic charge; this charge can be very important

to the conformational state and electrostatic properties of the protein, thus playing a role in protein function (5). An acetyl group neutralizes the charge of the lysine side chain potentially resulting in a local change in electrostatic properties around the modified lysine residue.

The removal of acetyl groups on modified lysine residues is performed by histone deacetylases (HDACs), which catalyze the hydrolysis of the acetyl groups producing a free amino groups once again. HDACs have been extensively investigated in their role in deacetylating histone proteins in the nucleus and other chromatin remodeling proteins involved in gene expression (6,7). The designation "histone" deacetylase, or "histone" acetyltransferase could be considered a misnomer due to the more recent investigative insight into the extent of acetylation throughout the cell, not only restricted to the nucleus (8,9,10). One could more generally categorize these enzymes as lysine deacetylases, or KDACs. Recently several ground breaking studies have been undertaken to understand the extent of acetylation on a proteomic scale (8,9,10). Mattias Mann's group and others have used large scale mass spectrometric approaches to determine that there are hundreds of different cytosolic and mitochondrial targets of acetylation, also that changes in cellular environment, nutrient availability, or HDAC inhibition can have large changes on acetylome patterns.

During tumorigenesis and cancer progression tumor cells become primarily glycosidic and must maintain growth and survival under stressful conditions (11). Solid tumors experience periods of low blood flow resulting in regions of the tumor being subjected to hypoxia and low glucose. Given the fact that tumor hypoxia is a clinical indicator for poor patient prognosis (12), tumor hypoxia could potentially select for tumor cells well adapted to survival and progression under metabolically difficult circumstances. This could allow these cells to go on to seed other lethal tumors. Some evidence (described in more detail in chapter 3) suggests that acetylation could

play a role in tumorigenesis and the ability of cancer cells to maintain high glycolysis and run-away growth. This is apparent in the many current clinical trials investigating general and specific HDAC inhibitors alone or in combination with other chemotherapy drugs as a means to treat various cancers (13).

Histone deacetylase 6 (HDAC6) is one such drug target that has been specifically targeted using small molecule inhibitors in cancer. HDAC6 is overexpressed in several cancer types (14) and is found primarily in the cytosol closely associated with the cytoskeleton. Indeed HDAC6 has been shown to directly deacetylate alpha-tubulin which promotes cytoskeletal stability (15). HDAC6 has been shown to be important in its role in promoting the unfolded protein response which is important to cell survival under stress conditions (16). HDAC6 has few known protein targets, which highlights the importance of finding targets for its deacetylase activity that could help to explain the oncogenic role of HDAC6. Further study of oncogenic acetylation regulation occurring in the cytosol has become an important question and one that will be addressed in this thesis.

The protein 14-3-3ζ is one such cytosolic protein that we have found to be regulated by acetylation pathways. 14-3-3ζ is one of seven isoforms of the 14-3-3 family of proteins. 14-3-3s have no known enzymatic properties but function by binding to other cellular proteins thereby modulating those proteins in a variety of different ways. 14-3-3s form homo- or heterodimers with other isoforms of 14-3-3 and bind to one or multiple proteins at the same time. 14-3-3 binds to phosphorylated proteins via interactions between positively charged amino acids (including lysines) within its binding pocket and the negatively charged phosphate of the binding partner. 14-3-3s are ubiquitously expressed in all eukaryotes and in all tissues being highly conserved between different isoforms and from different species. It has been suggested that because of the several

different genes for 14-3-3s that there is some functional specificity for the various isoforms of the protein. How much of each isoforms function overlaps with other isoforms is not known, though the formation of functional heterodimers suggests some overlap (17).

14-3-3ζ is a protein that generally promotes a pro-survival, pro-growth phenotype (18). Indeed 14-3-3ζ is overexpressed in many different types of cancer (19), and as will be shown in this work, 14-3-3ζ is more highly expressed in more aggressive breast cancer types. 14-3-3ζ exerts this phenotype by binding to and modulating the activity of critical proteins involved in apoptosis, cell cycle, and other cell fate determining pathways (20). It has been known for some time that the ability of 14-3-3ζ to bind to its target protein is usually determined by the phosphorylation status of the serine/threonine on the target protein binding motif (5). In this way 14-3-3ζ can be thought to act as a logic gate requiring the input of a kinase to allow 14-3-3ζ to complete its function (21). This type of phosphorylation regulation is well known and is ubiquitous in cell biology. Though, as has been previously stated, we have increased our understanding of the scope and importance of other PTM modifications, such as acetylation, in regulating cytosolic pathways. It has become increasingly important to develop better tools to better understand these complexities in protein regulation. Fortunately researchers have become highly skilled in analyzing protein lysine acetylation using mass spectrometry (7,8,9). With our improving methods and tools, it is becoming possible to screen complex cellular mixtures to monitor acetylation status. Analyzing the acetylation changes that occur during tumor formation has become an important question in how a cell might attain the necessary biochemical changes for tumor growth. Furthermore, if these pathways can be elucidated specific drug combinations may be developed to target cancer pathways on many fronts.

REFERENCES

1. Zhang, X.; Wen, H.; Shi, X. Lysine methylation: beyond histones. *Acta. Biochim. Biophys. Sin.* **2012**, 44, 1, 14- 27
2. Chen, L.; Li, Z.; Zwolinska, A.; Smith, M.; Cross, B.; Koomen J.; Yuan, Z. MDM2 recruitment of lysine methyltransferases regulates p53 transcriptional output. *EMBO J.* **2010**, 29, 2538–2552
3. Martin, D.; Beauchamp, E.; Berthiaume, L. Post-translational myristolation: fat matters in life and death. *Biochimie.* **2011**, 93, 18-31
4. Friedmann, D.; Marmorstein, R. Structure and mechanism of non-histone protein acetyltransferase enzymes. *FEBS J.* **2013**, 280, 22, 5570-81
5. Johnson, C.; Crowther, S.; Stafford, M. J.; Campbell, D. G.; Toth, R.; MacKintosh, C. Bioinformatic and experimental survey of 14-3-3 binding sites. *Biochem. J.* **2010**, 427, 69-78
6. Ropero, S.; Esteller, M. The role of histone deacetylases in human cancer. *Mol. Oncology.* **2007**, 1, 1, 19-25
7. Yang, X.; Gregoire, S. Class II histone deacetylases: from sequence to function, regulation, and clinical implication. *MCB.* **2005**, 25, 8, 2873-84
8. Choudhary, C.; Kumar, C.; Gnad, F.; Nielsen, M. L.; Rheman, M.; Walther, T. C.; Olsen, J. V.; Mann, M. Lysine acetylation targets protein complexes and co-regulates major cellular functions. *Science.* **2009**, 325, 5942, 834-40
9. Wang, W.; Zhang, Y.; Yang, C.; Xiong, H.; Lin, Y.; Yao, J. Acetylation of metabolic enzymes coordinates carbon source utilization and metabolic flux. *Science.* **2010**, 327, 5968, 1004-7
10. Zhao, S.; Xu, W.; Jiang, W.; Yu, W.; Lin, Y.; Zhang, T. Regulation of cellular metabolism by protein lysine acetylation. *Science.* **2010**, 327, 5968, 1000-4
11. Agbor, T. A.; Taylor, C. T. SUMO, hypoxia and the regulation of metabolism. *Biochemical Society transactions.* **2008**, 36, 3, 445-8
12. Wilson, W. R.; Hay, M. P. Targeting hypoxia in cancer therapy. *Nature Review Cancer.* **2011**, 11, 6, 791-804
13. West, A. C.; Johnstone, R. W. New and emerging HDAC inhibitors for cancer treatment. *J. Clinical Investigation*. **2014**, 124, 1, 30-39
14. Aldana-Masangkay, G.; Sakamoto, K. M. The role of HDAC6 in cancer. *J. Biomedicine and Biotechnology.* **2010**, 2011, doi:10.1155/2011/875824
15. Zhang, Y.; Li, N.; Caron, C.; Matthias, G.; Hess, D.; Khochbin, S.; Matthias. P. HDAC6 interacts with and deacetylates tubulin and microtubules in vivo. *EMBO.* **2003**, 22, 5, 1168-79
16. Kwon, S.; Zhang, Y.; Matthias, P. The deacetylase HDAC6 is a novel critical component of stress granules involved in the stress response. *Genes & Development.* **2007**, 21, 3381-94
17. Aitken, A.; Baxter, H.; Dubois, T.; Clokie, S.; Mackie, S.; Mitchell, K.; Peden, A.; Zemlickova, E. Specificity of 14-3-3 isoform dimer interactions and phosphorylation. *Biochem. Soc. Trans.* **2002**, 30, 4, 351-60
18. Yang, X.; Cao, W.; Zhang, L.; Zhang, W.; Zhang, X.; Lin, H. Targeting 14-3-3ζ in cancer therapy. *Cancer Gene Therapy.* **2012**, 19, 153-159
19. Li, Y.; Zou, L.; Li, Q.; Haibe-Kains, B.; Tian, R.; Li, Y.; Desmedt, C.; Sotiriou, C.; Szallasi, Z.; Iglehart, J. D.; Richardson, A. L.; Wang, Z. C. Amplification of LAPTM4B and YWHAZ

contributes to chemotherapy resistance and recurrence of breast cancer. *Nature Medicine.* **2010**, 16, 214-218
20. Kleppe, R.; Martinez, A.; Doskeland, S.; Haavik, J. The 14-3-3 proteins in regulation of cellular metabolism. *Sem. Cell. & Dev. Bio.* **2011**, 22, 713-719
21. Chen, S.; Synowsky, S.; Tinti, M.; MacKintosh, C. The capture of phosphoproteins by 14-3-3 proteins mediates actions of insulin. *Trends Endocrin. & Metab.* **2011**, 22, 11, 429-436

CHAPTER 2: HDAC6 IS NECESSARY FOR TUMOR CELL SURVIVAL DURING HYPOXIA

INTRODUCTION

Protein lysine acetylation is a reversible posttranslational modification (PTM) that is regulated by the activity of lysine acetyl-transferases (KATs) and lysine deacetylases (KDACs). Although acetylation approaches protein phosphorylation in terms of its scope across the proteome (1), our understanding of the mechanisms by which acetylation modulates cellular pathways is limited. Numerous *in vitro* studies targeting KDAC activity in cancer implicate lysine acetylation pathways in cell survival signaling (reviewed in (2)). Furthermore, the use of KDAC inhibitors in human cancer trials to enhance chemotherapy-induced tumor cell death implicate KDAC activity and protein acetylation as modulators of cell survival pathways *in vivo*. KDACs can be categorized based on their nuclear, cytosolic or mitochondrial localization. While the pro-survival function of nuclear KDACs is attributed to their modulation of histone acetylation and gene expression, the cytosolic and mitochondrial expression of several pro-survival KDACs and the high frequency of acetylation on cytosolic and metabolic proteins suggest that lysine acetylation may also regulate cell fate by modulating non-histone proteins and pathways (3-6).

Studies in both prokaryotes and mammalian cells suggest that changes in carbon source alter protein acetylation (3,5,7), which in turn can affect protein activity via several mechanisms, including allosteric regulation, direct interference with an enzyme's active site, or modulation of protein degradation (reviewed in (6)). In this sense, acetylation seems to be akin to other better-understood PTMs like phosphorylation in its ability to alter protein function in a variety of ways. Importantly, however, acetyl-CoA levels can be limiting for certain acetylation events (on histones for example), such that the level of protein acetylation tracks with acetyl-CoA levels (7,8). Indeed,

simply adding citrate to increase the cellular acetyl-CoA pool is sufficient to modulate protein acetylation and affect cell survival (7,9). Thus, the link between metabolic conditions, acetyl-CoA production, and changes in acetylation suggest that acetylation fits within a class of metabolite-derived PTMs (including lipidation and glycosylation) that may function as sensors to modulate core cellular pathways in response to changing nutrient levels.

Given the growing body of data implicating non-histone acetylation and cytosolic KDACs in metabolism and cell survival, we became interested in identifying pathways and mechanisms by which non-histone acetylation modulates cell survival. We chose to pursue these studies in the context of hypoxic stress (defined here as low glucose and low oxygen) given its frequent occurrence within solid tumors and its role in promoting chemoresistance (10). Using an acetyl-proteomics approach, we identified acetylation events across the proteome that changed dynamically under hypoxic conditions. Blunt perturbation of acetylation pathways with a KDAC inhibitor sensitized cells to hypoxia and further RNAi screening of all known human KDACs and KATs revealed specific modulators of cell fate in hypoxia. Prominent among the most significant hits in this screen was HDAC6, a cytosolic microtubule-associated deacetylase that regulates a variety of processes important to human disease, including cell survival, gluconeogenesis, cancer metastasis, and proteotoxicity (reviewed in (11)). For this reason, HDAC6 has recently emerged as a potential therapeutic target in cancer (12) and neurodegenerative disease (13). We found that inhibition of HDAC6, either via small molecule targeting or RNAi, potently sensitizes cells to hypoxia.

EXPERIMENTAL PROCEDURES

Cell culture-MDA-MB-231, MDA-MB-435, HEK-293T, and U2OS cells were purchased fro ATCC. All cell lines were maintained under sterile conditions using high glucose Dulbecco's

Cell culture-MDA-MB-231, MDA-MB-435, HEK-293T, and U2OS cells were purchased from ATCC. All cell lines were maintained under sterile conditions using high glucose Dulbecco's modified Eagle's Medium (DMEM purchased from Gibco) supplemented with 10% fetal bovine serum and 2 mM glutamine. The cells were cultured at 37°C in 5% CO_2/air. For all hypoxia treatments, cells were cultured in glucose-free DMEM (Gibco) supplemented with 2 mM glucose and cultured in a sterile hypoxia incubator at 37°C in 5% CO_2/air and 1% O_2.

Acetyl-proteomics and data analysis-Samples for acetyl-proteomics were generated by solubilization of cellular proteins, tryptic digestion, enrichment of acetyl-lysine (Kac) peptides, and LC-MS/MS analysis similar to previously described, with the exception that a pan-acetylK antibody (#11786BK) from Cell Signaling Technologies was utilized for the IP (20). Care was taken that the temperature not exceed 32°C throughout the procedure, to limit protein carbamylation by Urea. Briefly, samples were solubilized in 50 mM Ammonium Bicarbonate (AmBic, pH 8) containing 8 M Urea, then normalized to total protein content across all samples using a Bradford assay (Bio-Rad, Inc). The samples were reduced with 10 mM dithiothreitol at 32°C for 1 hr, followed by alkylation with 40 mM iodoacetamide for 1 hr in the dark. Samples were diluted to 1.8 M Urea with AmBic, then sequencing grade trypsin was added at a 1:25 w/w ratio and digestion proceeded overnight at 32°C. Samples were acidified to 1% TFA, buffer exchanged with Sep Pak C18 (Waters) and lyophilized to dryness. Peptides were resuspended in IAP Buffer (Cell Signaling Technologies) and incubated with a 40 ul aliquot of PTMScan Acetyl-K enrichment kit (11786BK) at 4C overnight. Enriched peptides were eluted with 1% TFA for 10 minutes, dried in a speed-vac, and resuspended in 12 ul 1/2/97 v/v/v TFA/MeCN/water containing a total of 50 fmol ADH1_YEAST digest (Waters Corporation). LC-MS/MS analysis took place on a nanoAcquity UPLC coupled via electrospray to a LTQ Orbitrap XL mass spectrometer exactly

as previously described (20). Database searching for peptide identifications utilized Mascot v2.2 (Matrix Sciences), searching the Uniprot ('reviewed') database (www.uniprot.org) with *homo sapiens* taxonomy, searching the data with 10 ppm precursor and 0.8 Da product ion tolerance, and allowing for variable modifications deamidation (NQ), oxidation (M), and acetylation (K). Quantitative data were processed in Rosetta Elucidator v3.3, allowing relative quantification of all peptides identified in this dataset based on extracted ion chromatograms (peak areas) and accurate-mass and retention time alignment.

SRB assays-For 14-3-3ζ expression via plasmid transfection, HEK-293T cells were plated in 6-cm dishes at approximately 60% confluency. After transfection, cells were trypsinized and plated in 96-well plates at 30% confluency. Cells were treated with Tubacin (ranged from 10 μM to 80 μM) in combination with hypoxia (1% O_2, 2 mM glucose) for 48 hours. MDA-MB-435 cells were plated in 96-well plates at a density of 25% initial confluency before siRNA transfection. After 24 hours of siRNA treatment, cells were treated with hypoxia for 48 hours. Following hypoxia treatment, all 96-well plates were assayed using G Biosciences CytoScan SRB Cytotoxicity Assay kit (G Biosciences, St. Louis, MO, USA) according to the manufacturer's protocol. Absorbance values for each treated well were normalized using control untreated wells grown on the same plates. Cytotoxicity was calculated as 100*(Absorbance control - Absorbance treated)/Absorbance control.

Flow cytometry-MDA-MB-435 or U2OS cells were initially plated in 6-well plates at 20-30% confluence (20% for siRNA transfected cells and 30% for Tubacin treated cells). After 24 hours, cells were treated with either siRNA transfection followed by 48 hours of hypoxia, or 48 hours of a Tubacin (10 μM) and hypoxia combination treatment. HEK-293 cells were plated in 6-cm dishes at a confluency of 75%. Cells were then transfected with HA-14-3-3ζ WT or RR mutant

expression plasmid. HEK cells were then trypsinized and plated in 6-well plates at 30% initial confluency followed by 48 hours of a Tubacin (10-40 μM) and hypoxia combination treatment. Following treatment, the 6-well plates were prepared for flow cytometry analysis. Briefly, cells were trypsinized then washed with cold PBS. Next, cells were resuspended in cold PBS with 0.2% FBS and 1 μg/ml propidium iodide. Cells were analyzed for cell death using BD Facs Canto system.

Western blotting-MDA-MB-231, MDA-435, U2OS, cells were plated in 6 well plates at 75% confluency followed by siRNA transfection or drug treatments. Cells treated with siRNA HDAC6 knockdown were transfected with siRNA 12 hours after 14-3-3ζ transfection and allowed to grow for 36 hours. Following drug treatment or siRNA transfection, cells were lysed in an ice-cold Amandas coIP buffer (10 mM HEPES pH 7.5, 150 mM KCl, 0.1% NP-40, 10 mM beta-glycerophosphate, protease inhibitor cocktail). Cell lysates were centrifuged at 21000xg for 10 minutes, supernatant samples were boiled with SDS sample buffer (10% SDS, 30% glycerol, 0.7 M beta-mercaptoethanol, 0.15 M Tris, Bromophenol Blue). 40 μg of each sample was loaded and separated on 10-12% polyacrylamide gels. Western blots were visualized on LiCor Odyssey system (Lincoln, NE, USA).

Antibodies-Antibodies used: HDAC6 (#7612S) purchased from Cell Signaling Technology (Beverly, MA, USA), Actin (sc-1616-R) purchased from Santa Cruz Biotechnology (Dallas, TX, USA); HDAC1 provided by Dr. Srividya Bhaskara (University of Utah, USA).

siRNA and plasmid transfections-HEK-293 and U2OS cells were transfected with plasmid expression vectors pcDNA3.1 HA-14-3-3ζ, HA-Atg9 (gift from Luigi Puglielli at the University of Wisconsin using Turbofect transfection reagent and protocol (#R531, Thermo Scientific, Rockford, IL, USA). MDA-MB-435, U2OS, and HEK-293 cells were transfected with smartpool

siRNA from Dharmafect (Thermo Scientific, Rockford, IL, USA) using RNAiMax Lipofectamine reagent and protocol (Invitrogen, Rockford, IL, USA).

RESULTS

Perturbation of acetylation dynamics sensitizes cells to metabolic stress-To gain a better understanding of the underlying proteome-wide changes in acetylation occurring in hypoxia, we pursued an acetyl-proteomics approach (1). Of note, "hypoxia" in our experiments refers to *in vitro* conditions that mimic the ischemia commonly found within solid tumors, in which both oxygen *and* glucose are limited. Three cell lines were chosen for analysis: MDA-MB-231s and MDA-MB-435s, which we had previously characterized as being relatively sensitive and resistant, respectively, to hypoxia-induced cell death. In addition, we chose HEK-293s as a third cell line for comparison. Prior to proteomics analysis, cells were treated with hypoxia (1% O_2, 2mM glucose) for 3 hours or left in normoxia (atmosopheric O_2, 20 mM glucose). Affinity purification of acetylated peptides and LC-MS/MS analysis revealed approximately 658 different acetylation sites, representing 303 acetylated proteins. Using label-free quantification to measure relative abundance of these acetylated peptides under hypoxic or normoxic conditions across the three cell lines, we found that HEK-293 cells showed the highest magnitude change in acetylation between treatments, while MDA-MB-231 and MDA-MB-435 cells showed lower magnitude changes in acetylation, respectively (Fig 1A). Replotting these data as a 2D hierarchical cluster across all acetylated peptides and cell lines also shows the highest correlation in acetylation change between hypoxic and normoxic cells first within a given cell line, then between MDA-MB-231 and MDA-MB-435, then finally within HEK-293 cells. These changes are depicted in Figure 1C.

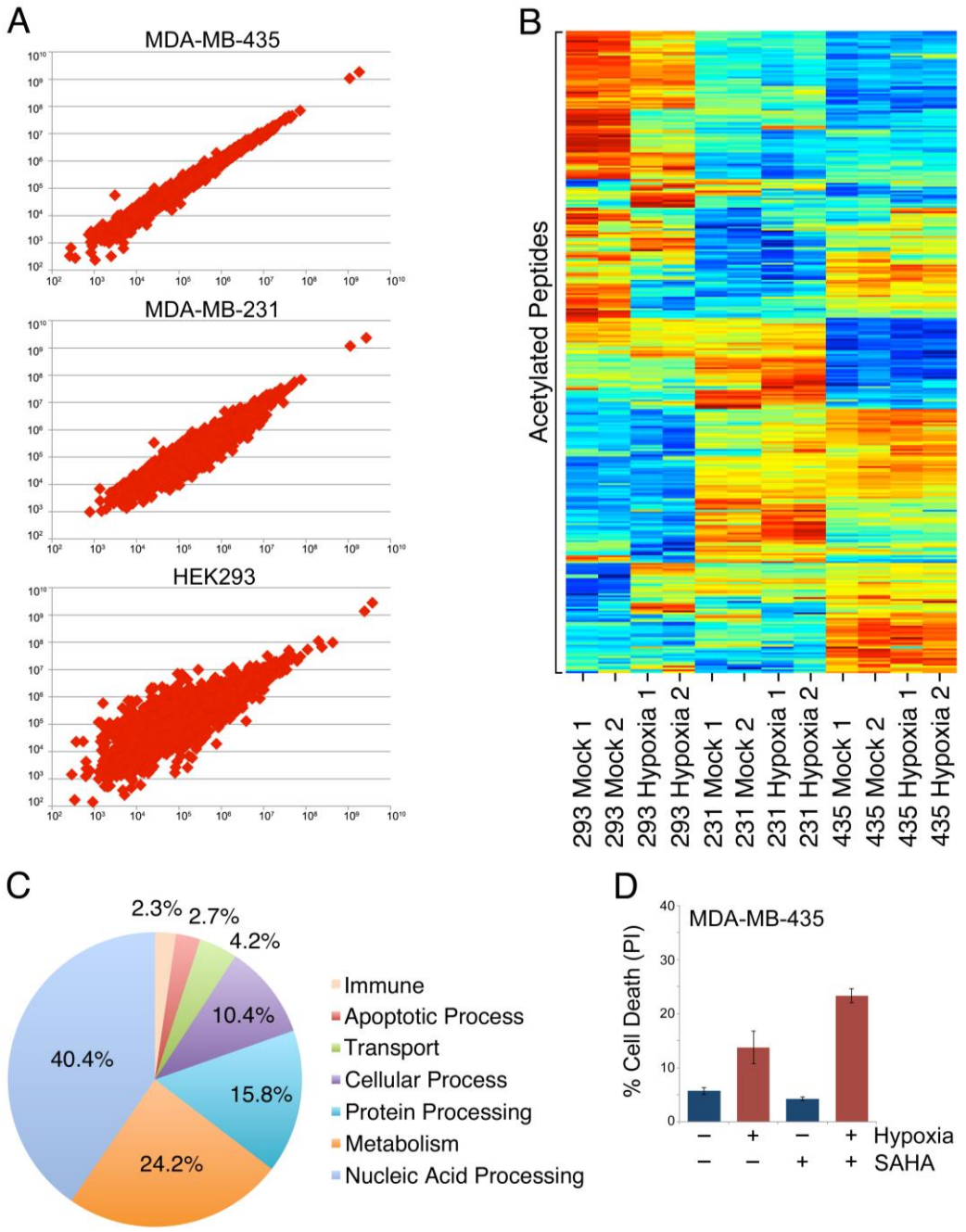

Figure 1. Oxygen and glycose limitation induces changes in acetylation across the proteome. (**A**) Acetyl-proteomic profiling was performed using MDA-MB-435, MDA-MB-231, and HEK293 cell lines. Cells were incubated under normal cell culture conditions or treated with 2mM glucose and 1% O_2 for three hours. Acetyl-peptide intensities from all cell lines were quantified using Elucidator software, which is represented as ratio dot plots (normoxic peak intensities on y-axis and correlating hypoxic peak intensities on x-axis). (**B**) Data from all cell lines and treatments were replotted as a 2D hierarchical cluster. Labels of 1 and 2 represent different runs on the mass spectrometer. (**C**) Acetyl-peptides were categorized by parent proteins using Panther GO annotation software and grouped according to biological activity and pathway. (**D**) MDA-MB-435 breast cancer cells were treated with 100 nM SAHA or vehicle (DMSO) and normoxic or hypoxic conditions (2mM glucose and 1% O_2) for 48 hours. Cell death was measured by PI staining and flow cytometry (mean±SEM, n=3).

Further categorization of all acetyl-lysine peptides from the LC-MS/MS analysis according to biological process showed that a large proportion of the targets were associated with nucleic acid processing, core metabolic pathways, and protein metabolism (Fig 1B). A subset of cancer-associated proteins that showed a hypoxia-triggered change in acetylation is highlighted in **Table 1**. Given that MDA-MB-435s showed very little change in acetylation in hypoxia and appeared relatively insensitive to hypoxic stress, we were interested in determining whether blunt perturbation of acetylation pathways with a KDAC inhibitor (KDACi) could sensitize these cells to hypoxia. MDA-MB-435 cells were treated with the pan-KDACi suberoylanilide hydroxamic acid (SAHA) at low concentrations to minimize off-target effects of the drug. Under these conditions, we observed a significant increase in hypoxia-induced death in SAHA-treated cells (Fig 1D) with very low toxicity in normoxic cells, suggesting that interfering with acetylation at the level of acetylation *turnover* sensitizes cells to hypoxia.

Table 1. Summary of selected acetylated lysine peptides. A subset of proteins that displayed changes in acetylation under hypoxic conditions. Lysine position, acetylation intensity fold change in hypoxia, and other known PTMs are shown.

Parent Protein	Position	Hypoxia (Elucidator)	(Uniprot.org)	(Phosphosite.org)
Phosphoglycerate kinase-1	K199	2.90	Acetyl	Acetyl, Ubiquitin
Phosphatidylinositide-dependent kinase-1	K304	2.15	None	Acetyl, Ubiquitin
Lactate dehydrogenase-A	K5	1.67	Acetyl	Acetyl, Ubiquitin, Succinyl
	K81	-1.46	Acetyl	Acetyl, Ubiquitin, Succinyl
	K118	2.06	Acetyl	Acetyl, Ubiquitin, Succinyl
Fatty acid synthase	K646	3.53	None	Acetyl
	K673	-1.53	Acetyl	Acetyl, Ubiquitin, Succinyl
	K1704	-1.97	Acetyl	Acetyl, Ubiquitin
	K1752	-1.55	None	Acetyl, Ubiquitin
	K1771	-2.22	Acetyl	Acetyl
Malate dehydrogenase (mitochondrial)	K335	-2.07	Acetyl	Acetyl, Succinyl
Pyruvate kinase type M2	K367	-1.40	None	Acetyl, Ubiquitin
c-Myc	K148	-1.98	Acetyl	Acetyl, Ubiquitin
PARP	K97	-2.15	Acetyl	Acetyl
	K108	-1.45	None	Acetyl, Ubiquitin
	K621	-1.86	Acetyl	Acetyl, Ubiquitin
Glucose-6-phosphate isomerase	K454	-1.42	Malonyl	Acetyl, Ubiquitin, Succinyl

Screening reveals HDAC6 as a regulator of cell survival in hypoxia-Given these results, we became interested in identifying specific acetylation-regulating enzymes that modulate cell survival under conditions of metabolic stress. Therefore we used an RNAi screening approach in

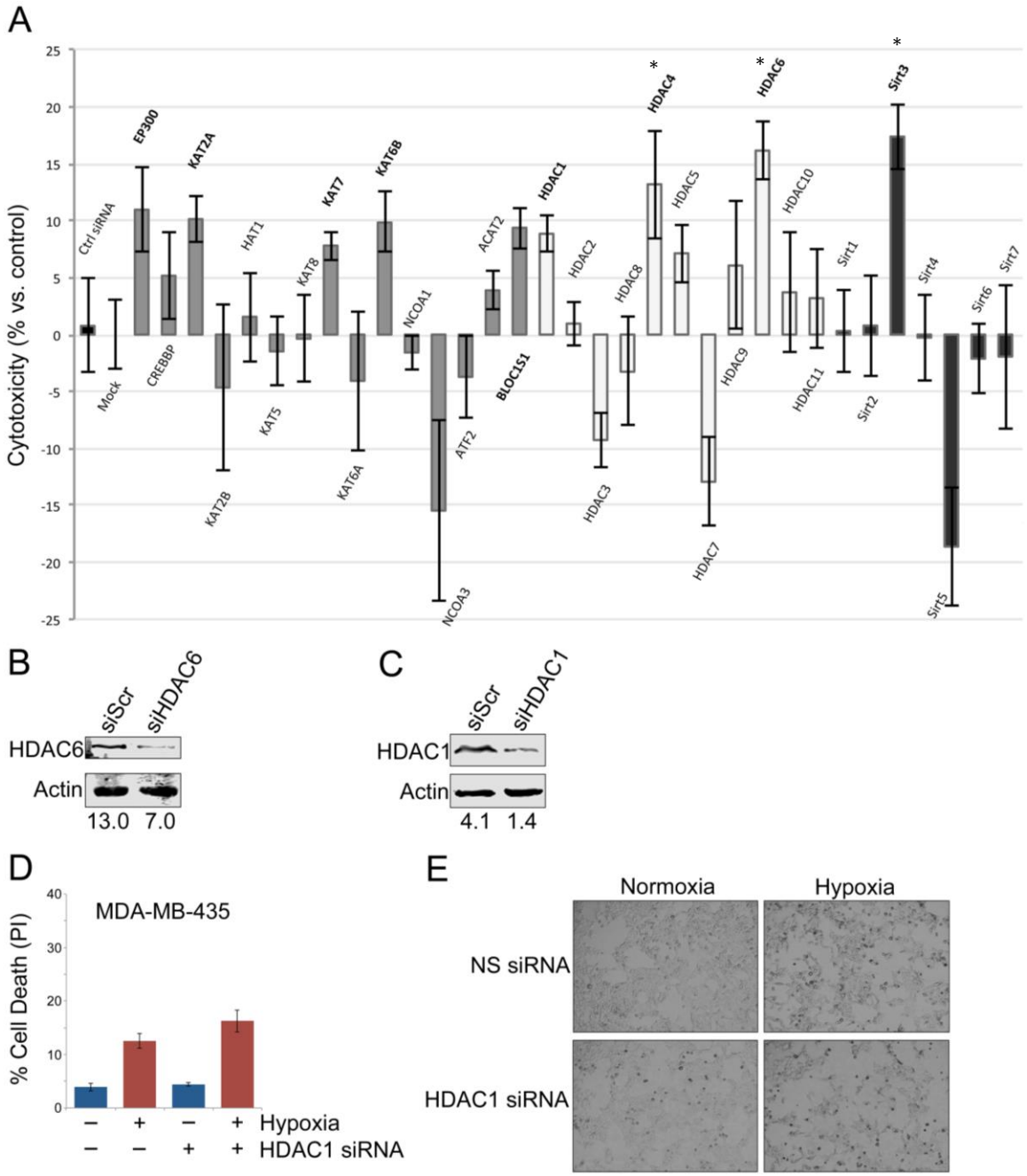

Figure 2. RNAi screen identifies acetylation-regulating enzymes required for cell survival in hypoxia. (**A**) MDA-MB-435 breast cancer cells were transfected with 75 nM siRNA against all human KATs and KDACs (custom smart pool library, Dharmacon), followed by exposure to hypoxia for 48 hours. Total cellular content was measured using absorbance-based SRB assay. Cytotoxicity (% vs. control) was calculated against mock-treated cells (mean±SEM, n=3, *indicates p-value<0.05). (**B**) Representative Western blot of HDAC6 knockdown using siRNA from library. Numbers below blots represent the intensity of HDAC6 normalizd to Actin as quantified by LI-COR infrared imaging. (**C**) Representative immunoblot of HDAC1 knockdown using siRNA from library. Bands were quantified as in panel B. (**D**) MDA-MB-435 cells were transfected with smartpool HDAC1 siRNA or scrambled siRNA and exposed to normoxic or hypoxic conditions for 48 hours. Cell death was measured by PI staining and flow cytometry. Data represented as bar graph (mean±SEM, n=3), or (**E**) Light microscope images.

which MDA-MB-435 cells were transfected with siRNA from a custom library targeted against known human KDACs and KATs, followed by hypoxia treatment and measurement of cell viability. For our initial assessment of viability we used an SRB cytotoxicity assay, which measures cellular content in each well. Follow-up assays using propidium iodide staining and flow cytometry to quantify cell death were used to validate selected hits. Four separate experiments are summarized in Figure 2A. Several KDAC-targeted siRNAs caused a significant decrease in cell viability, with depletion of HDAC4, HDAC6 and Sirt3 showing the highest magnitude cytotoxicity in the screen (Fig 2A). The HDAC4 and Sirt3 results are corroborated by published studies showing that HDAC4 positively regulates HIF-1a activation (22), and Sirt3 is required for cell survival in hypoxia (23). Figures 2D, E and 3A show further validation of HDAC1 and HDAC6 as pro-survival factors in hypoxia. Consistent with the SRB data in Figure 2A, Depletion of HDAC1 had a moderate effect on cell survival in hypoxia (Fig 2D,E), while depletion of HDAC6 potently enhanced hypoxia-induced cell death (Fig 3A-D). Further targeting of HDAC6 with the selective inhibitor Tubacin sensitized both MDA-MB-435s and the osteosarcoma cell line U20S to hypoxia-induced death (Fig 3E-G). Taken together, these data suggest that perturbation of lysine acetylation pathways via selective inhibition of individual deacetylases, including the non-histone deacetylase HDAC6, sensitizes cells to metabolic stress.

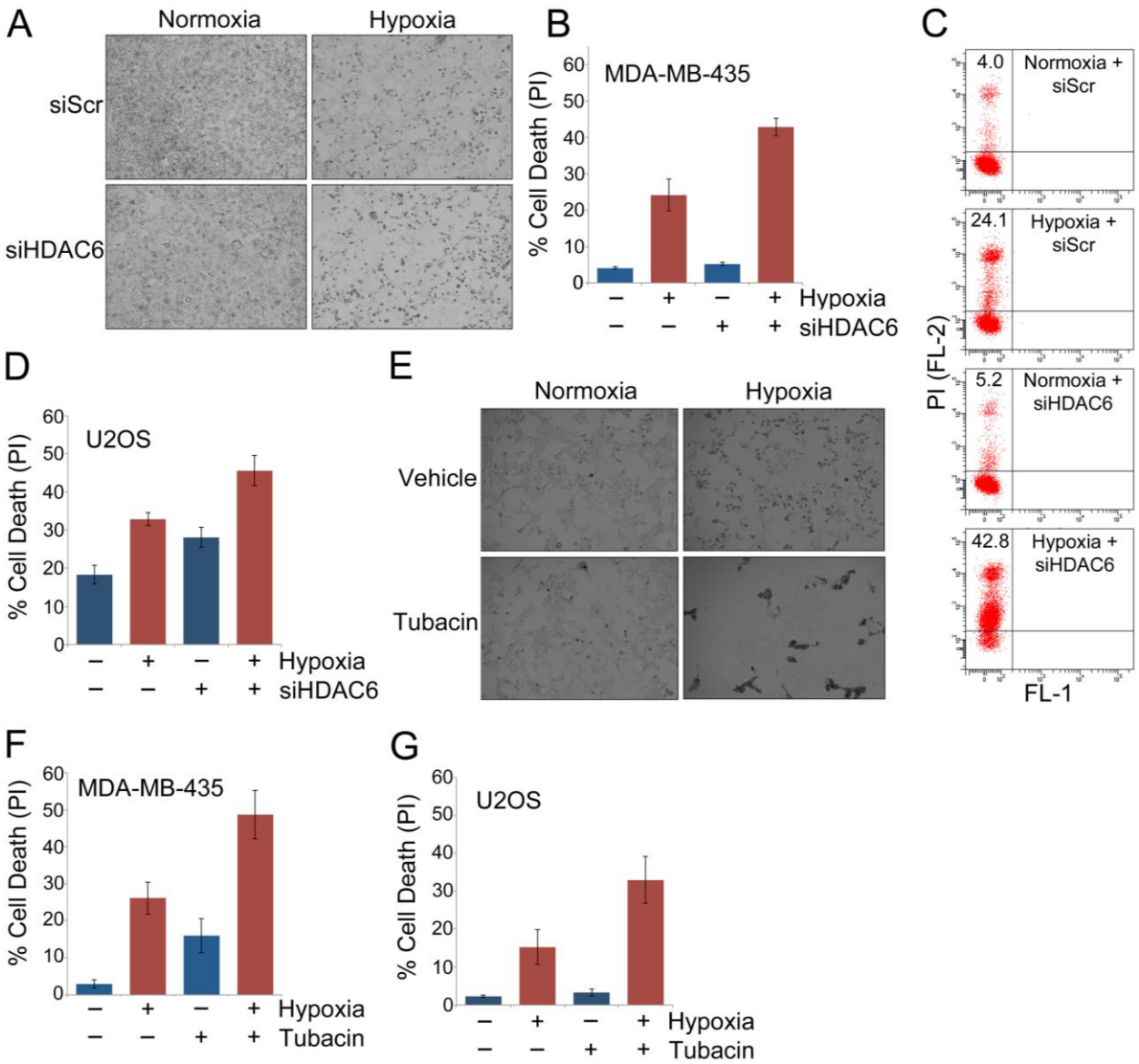

Figure 3. Inhibition of HDAC6 sensitizes cells to hypoxia. (**A**) MDA-MB-435 cells were transfected with 75 nM smartpool HDAC6 siRNA or scrambled siRNA and exposed to normoxic or hypoxic conditions for 48 hours. Cell death was measured by PI staining and flow cytometry. Data represented as light microscope pictures, or (**B**) Bar graph (mean±SEM, n=3), or (**C**) Flow cytometry dot plots. (**D**) U2OS cells were transfected with smartpool 75 nM HDAC6 siRNA or scrambled siRNA and exposed to normoxic or hypoxic conditions for 48 hours. Cell death was measured by PI staining and flow cytometry. Data represented as bar graph (mean±SEM, n=3), or (**E**) Light microscope pictures. (**F**) MDA-MB-435 cells were treated with a combination treatment of tubacin (10 μM) or vehicle and normoxic or hypoxic conditions for 48 hours. Cell death was measured by PI staining and flow cytometry. Data from three replicate experiments is presented as a bar graph (mean±SEM, n=3). (**G**) U2OS cells were treated in same manner as in figure 3F. Cell death was measured by PI staining and flow cytometry. Data represented as bar graph (mean±SEM, n=3).

DISCUSSION

While the acetylation of histones was discovered nearly a half century ago (31), the occurrence of acetylation on non-histone proteins has been a relatively recent finding (32). The rapid development and improvement of acetyl-proteomics methodologies within the last 6 years has led to the discovery of hundreds of acetylated proteins across the mitochondrial and cytosolic proteomes (1,3,5). In addition, the last decade has brought a greater understanding of the diversity within the HDAC and Sirtuin deacetylase families, revealing several deacetylases that primarily regulate non-histone substrates. These include Sirt2, Sirt3 (a mitochondrial deacetylase), HDAC6 and HDAC10. Furthermore, HDACs and Sirtuins initially thought to be strictly nuclear deacetylases (e.g., HDAC3, HDAC4 and Sirt1) have been shown to shuttle between the nucleus and cytoplasm and target non-histone proteins (reviewed in (33)). However, the functional consequences of non-histone acetylation remain poorly understood.

Two lines of evidence motivated us to look at acetylation dynamics in the context of low glucose/oxygen metabolic stress. First, changes in carbon source have been shown to modulate acetylation levels of non-histone proteins (3,5). Second, the manipulation of acetyl-CoA levels, which is known to affect protein acetylation (7,8), has been shown to modulate core regulators of cell survival (9). Based on these data, we posited that acetylation-regulated pathways might play a critical role in survival under conditions that mimic tumor hypoxia, in which cells are forced to shift their metabolism from glucose to alternative carbon sources (34). Indeed, our acetyl-proteomics studies revealed changes in acetylation in response to hypoxia, and perturbation of acetylation turnover via KDAC inhibition sensitized cells to hypoxia-induced death. Interestingly, while we observed a slight trend toward an overall decrease in acetylation in hypoxic cells, many lysines showed increased acetylation—suggesting that changes in acetylation under these

conditions are not simply a function of acetyl-CoA levels, but may reflect changes in KAT and/or KDAC activity. Together, our data demonstrate that the activity of HDAC6 is critical for suppressing cell death under conditions of metabolic stress.

REFERENCES

1. Choudhary, C., Kumar, C., Gnad, F., Nielsen, M. L., Rehman, M., Walther, T. C., Olsen, J. V., and Mann, M. S*cience.* **2009**, 325, 834-840
2. Khan, O., and La Thangue, N. B. *Immunology and cell biology.* **2012**, 90, 85-94
3. Wang, Q., Zhang, Y., Yang, C., Xiong, H., Lin, Y., Yao, J., Li, H., Xie, L., Zhao, W., Yao, Y., Ning, Z. B., Zeng, R., Xiong, Y., Guan, K. L., Zhao, S., and Zhao, G. P. *Science.* **2010**, 327, 1004-1007
4. Hirschey, M. D., Shimazu, T., Goetzman, E., Jing, E., Schwer, B., Lombard, D. B., Grueter, C. A., Harris, C., Biddinger, S., Ilkayeva, O. R., Stevens, R. D., Li, Y., Saha, A. K., Ruderman, N. B., Bain, J. R., Newgard, C. B., Farese, R. V., Jr., Alt, F. W., Kahn, C. R., and Verdin, E. *Nature.* **2010**, 464, 121-125
5. Zhao, S., Xu, W., Jiang, W., Yu, W., Lin, Y., Zhang, T., Yao, J., Zhou, L., Zeng, Y., Li, H., Li, Y., Shi, J., An, W., Hancock, S. M., He, F., Qin, L., Chin, J., Yang, P., Chen, X., Lei, Q., Xiong, Y., and Guan, K. L. *Science.* **2010**, 327, 1000-1004
6. Xiong, Y., and Guan, K. L. *The Journal of cell biology.* **2012**, 198, 155-164
7. Wellen, K. E., Hatzivassiliou, G., Sachdeva, U. M., Bui, T. V., Cross, J. R., and Thompson, C. B. *Science.* **2009**, 324, 1076-1080
8. Cai, L., Sutter, B. M., Li, B., and Tu, B. P. *Molecular cell.* **2011**, 42, 426-437
9. Yi, C. H., Pan, H., Seebacher, J., Jang, I. H., Hyberts, S. G., Heffron, G. J., Vander Heiden, M. G., Yang, R., Li, F., Locasale, J. W., Sharfi, H., Zhai, B., Rodriguez-Mias, R., Luithardt, H., Cantley, L. C., Daley, G. Q., Asara, J. M., Gygi, S. P., Wagner, G., Liu, C. F., and Yuan, J. *Cell.* **2011**, 146, 607-620
10. Wilson, W. R., and Hay, M. P. *Nature reviews. Cancer.* **2011**, 11, 393-410
11. Yang, P. H., Zhang, L., Zhang, Y. J., Zhang, J., and Xu, W. F. *Drug discoveries & therapeutics.* **2013**, 7, 233-242
12. Santo, L., Hideshima, T., Kung, A. L., Tseng, J. C., Tamang, D., Yang, M., Jarpe, M., van Duzer, J. H., Mazitschek, R., Ogier, W. C., Cirstea, D., Rodig, S., Eda, H., Scullen, T., Canavese, M., Bradner, J., Anderson, K. C., Jones, S. S., and Raje, N. *Blood.* **2012**, 119, 2579-2589
13. Pandey, U. B., Nie, Z., Batlevi, Y., McCray, B. A., Ritson, G. P., Nedelsky, N. B., Schwartz, S. L., DiProspero, N. A., Knight, M. A., Schuldiner, O., Padmanabhan, R., Hild, M., Berry, D. L., Garza, D., Hubbert, C. C., Yao, T. P., Baehrecke, E. H., and Taylor, J. P. *Nature.* **2007**, 447, 859-863
14. Aldana-Masangkay, G. I., and Sakamoto, K. M. *Journal of biomedicine & biotechnology.* **2011**, 2011, 875824
15. Li, Z., Zhao, J., Du, Y., Park, H. R., Sun, S. Y., Bernal-Mizrachi, L., Aitken, A., Khuri, F. R., and Fu, H. *Proceedings of the National Academy of Sciences of the United States of America.* **2008**, 105, 162-167
16. Lu, J., Guo, H., Treekitkarnmongkol, W., Li, P., Zhang, J., Shi, B., Ling, C., Zhou, X., Chen, T., Chiao, P. J., Feng, X., Seewaldt, V. L., Muller, W. J., Sahin, A., Hung, M. C., and Yu, D. *Cancer cell.* **2009**, 16, 195-207
17. Maxwell, S. A., Li, Z., Jaye, D., Ballard, S., Ferrell, J., and Fu, H. *The Journal of biological chemistry.* **2009**, 284, 22379-22389

18. Neal, C. L., Yao, J., Yang, W., Zhou, X., Nguyen, N. T., Lu, J., Danes, C. G., Guo, H., Lan, K. H., Ensor, J., Hittelman, W., Hung, M. C., and Yu, D. *Cancer research.* **2009**, 69, 3425-3432
19. Neal, C. L., and Yu, D. *Expert opinion on therapeutic targets.* **2010**, 14, 1343-1354
20. Iwabuchi, M., Sheng, H., Thompson, J. W., Wang, L., Dubois, L. G., Gooden, D., Moseley, M., Paschen, W., and Yang, W. *Journal of cerebral blood flow and metabolism : official journal of the International Society of Cerebral Blood Flow and Metabolism.* **2014**, 34, 425-432
21. Goto, H., and Inagaki, M. *Nature protocols.* **2007**, 2, 2574-2581
22. Geng, H., Harvey, C. T., Pittsenbarger, J., Liu, Q., Beer, T. M., Xue, C., and Qian, D. Z. *The Journal of biological chemistry.* **2011**, 286, 38095-38102
23. Pellegrini, L., Pucci, B., Villanova, L., Marino, M. L., Marfe, G., Sansone, L., Vernucci, E., Bellizzi, D., Reali, V., Fini, M., Russo, M. A., and Tafani, M. *Cell death and differentiation.* **2012**, 19, 1815-1825
24. Andersen, J. L., Thompson, J. W., Lindblom, K. R., Johnson, E. S., Yang, C. S., Lilley, L. R., Freel, C. D., Moseley, M. A., and Kornbluth, S. *Molecular cell.* **2011**, 43, 834-842
25. Ge, F., Li, W. L., Bi, L. J., Tao, S. C., Zhang, Z. P., and Zhang, X. E. *Journal of proteome research.* **2010**, 9, 5848-5858
26. Pozuelo-Rubio, M. *The FEBS journal.* **2010**, 277, 3321-3342
27. Molzan, M., Kasper, S., Roglin, L., Skwarczynska, M., Sassa, T., Inoue, T., Breitenbuecher, F., Ohkanda, J., Kato, N., Schuler, M., and Ottmann, C. *ACS chemical biology.* **2013**, 8, 1869-1875
28. Masters, S. C., and Fu, H. *The Journal of biological chemistry.* **2001**, 276, 45193-45200
29. Matta, A., Siu, K. M., and Ralhan, R. *Expert opinion on therapeutic targets.* **2012**
30. Yang, X., Cao, W., Zhang, L., Zhang, W., Zhang, X., and Lin, H. *Cancer gene therapy.* **2012**, 19, 153-159
31. Phillips, D. M. *The Biochemical journal* **1963**, 87, 258-263
32. Kim, S. C., Sprung, R., Chen, Y., Xu, Y., Ball, H., Pei, J., Cheng, T., Kho, Y., Xiao, H., Xiao, L., Grishin, N. V., White, M., Yang, X. J., and Zhao, Y. *Molecular cell.* **2006**, 23, 607-618
33. Yao, Y. L., and Yang, W. M. *Journal of biomedicine & biotechnology.* **2011**, 2011, 146493
34. Wise, D. R., Ward, P. S., Shay, J. E., Cross, J. R., Gruber, J. J., Sachdeva, U. M., Platt, J. M., DeMatteo, R. G., Simon, M. C., and Thompson, C. B. **2011**

CHAPTER 3: HISTONE DEACETYLASE 6 (HDAC6) PROMOTES THE PRO-SURVIVAL ACTIVITY OF 14-3-3ζ VIA DEACETYLATION OF LYSINES WITHIN THE 14-3-3ζ BINDING POCKET

INTRODUCTION

The 14-3-3 protein family includes seven human isoforms that regulate diverse processes, including metabolism, cell cycle control, protein trafficking, cell motility, and apoptosis. While these functions are somewhat dispersed between the different isoforms, the zeta (ζ) isoform plays a prominent role in promoting cell growth and survival pathways (1). Like other 14-3-3 isoforms, 14-3-3ζ functions by binding to and modulating the activity of a large network of serine/threonine-phosphorylated proteins. Depending on the phosphorylated protein in question, the effect of 14-3-3ζ binding varies from activation, suppression, sequestration, or scaffold-like activity.

14-3-3ζ coordinates the activation of several well-characterized oncogenic, metabolic, and pro-survival pathways. For example, in response to insulin, 14-3-3ζ binds to the AKT-phosphorylated GTPase protein AS160. This insulin-dependent binding event promotes translocation of the glucose transporter GLUT4 to the plasma membrane (2). Once inserted into the membrane, GLUT4 is active and supports Warburg metabolism and proliferation in breast cancer and multiple myeloma (3-5). As another example, in response to glucose, 14-3-3ζ interacts with and suppresses Bad, a critical BH3-only protein required for chemotherapy-induced apoptosis (6-9). 14-3-3ζ expression also promotes epithelial to mesenchymal transition (EMT) by cooperating with HER2 in breast cancer (10), enhances anchorage-independent growth (11,12), and suppresses anoikis (12). Many of these phenotypes have been attributed to 14-3-3ζ-mediated regulation of the TGF-β/Smads, IGF1R, PI3K/AKT, and β-catenin pathways (reviewed in (13)). Furthermore, 14-3-3ζ interacts with and suppresses both Caspase-2 (14,15) and the Forkhead

family member FKHRL1, preventing the expression of the pro-apoptotic Bax and Fas proteins (16).

Clinical studies demonstrate a correlation between high 14-3-3ζ expression and poor prognosis in several cancer types, including lung, head and neck, glioblastoma, and breast cancer (10-13,17,18). Furthermore, Bergamaschi et al. demonstrated that high 14-3-3ζ expression is positively correlated with breast tumor relapse, metastasis, tamoxifen treatment, and tamoxifen resistance (19). Moreover, we show here that 14-3-3ζ expression is particularly high in the more aggressive breast cancer subtypes and in tumors with negative receptor status. In support of an oncogenic function for 14-3-3ζ, others have shown that the depletion of 14-3-3ζ suppresses proliferation and enhances chemosensitivity in xenografted breast tumors (10,11). Based on this rationale, several groups have attempted to develop 14-3-3ζ inhibitors (reviewed in (20,21), Andersen unpublished), but no 14-3-3ζ-directed therapeutic strategies are currently being used in the clinic.

The current paradigm of 14-3-3ζ regulation states that 14-3-3ζ interactions depend primarily on the serine/threonine phosphorylation of binding partners—thus, phosphorylation of binding partners is considered a major determinant of 14-3-3ζ binding activity. Comparatively little is known about other potential determinants of 14-3-3ζactivity (22-25). In search of post-translational modifications that regulate 14-3-3ζ directly, we identified several lysines on 14-3-3ζ that are modified by acetylation. Lysine-to-glutamine (K-to-Q) mutations at two of these lysines, K49 and K120, abolish 14-3-3ζ binding activity. In an effort to modulate 14-3-3ζ binding via acetylation, we developed site-specific antibodies to both acetyl-K49 and acetyl-K120 and identified HDAC6 as the 14-3-3ζ-targeted deacetylase.

Recent studies implicate HDAC6 as a therapeutic target in cancer (26-29), and our data suggest that HDAC6 inhibition may provide a means to inhibit 14-3-3ζ. Toward this end, we show that inhibition of HDAC6 triggers dissociation of 14-3-3ζ from AS160 and Bad, two well-characterized binding partners. We also show that these dissociation events lead to decreased AS160 T642 and Bad S112 phosphorylation. Importantly, the loss of interaction and phosphorylation due to HDAC6 inhibition is rescued by an acetylation-refractory lysine-to-arginine (K-to-R) mutant of 14-3-3ζ. Together, our data suggest a model in which 14-3-3ζ activity is governed by the balance between K49/K120-targeted deacetylase activity and acetyl-transferase activity. We posit that under normal growth conditions, 14-3-3ζ acetylation is maintained at a very low level by HDAC6, allowing deacetylated 14-3-3ζ to bind and modulate its network of interacting proteins. However, upon HDAC6 inhibition, acetylation of 14-3-3ζ promotes dissociation of 14-3-3ζ-protein complexes, resulting in a loss of 14-3-3ζ-mediated growth and survival signaling.

EXPERIMENTAL PROCEDURES

Cell culture and reagents – MDA-MB-231, HEK-293T, and U2OS cells were purchased from ATCC. All cell lines were maintained under sterile conditions using high glucose Dulbecco's modified Eagle's medium (DMEM; purchased from Gibco) supplemented with 10% fetal bovine serum and 2 mM glutamine. The cells were cultured at 37°C in 5% CO_2/air. HDAC inhibitor drugs SAHA, Trichostatin A, Salermide, Ex-527, Tubacin, and Tubastatin A were purchased from Cayman Chemical (Ann Arbor, Michigan, USA). Drugs applied to cell culture were first dissolved in DMSO and then added to culture media to the final concentrations indicated.

siRNA and plasmid transfections – HEK-293T and U2OS cells were transfected with plasmid expression vectors pcDNA3.1 HA-14-3-3ζ HA-Atg9 (gift from Dr. Luigi Puglielli at the University of Wisconsin), FLAG-AS160 (gift from Dr. Gus Lienhard at Dartmouth University), and Bad using Turbofect transfection reagent and protocol (#R531, Thermo Scientific, Rockford, IL, USA). Site-specific mutants of HA-14-3-3ζ were produced using Agilent Quickchange kit (Santa Clara, California, USA). U2OS and HEK-293T cells were transfected with smartpool siRNA from Dharmafect (Thermo Scientific, Rockford, IL, USA) using RNAiMAX Lipofectamine reagent and protocol (Invitrogen, Rockford, IL, USA).

Acetyl-proteomics and data analysis-Samples for acetyl-proteomics were generated by solubilization of cellular proteins, tryptic digestion, enrichment of acetyl-lysine (Kac) peptides, and LC-MS/MS analysis similar to previously described, with the exception that a pan-acetylK antibody (#11786BK) from Cell Signaling Technologies was utilized for the IP (20). Care was taken that the temperature not exceed 32°C throughout the procedure, to limit protein carbamylation by Urea. Briefly, samples were solubilized in 50 mM Ammonium Bicarbonate (AmBic, pH 8) containing 8 M Urea, then normalized to total protein content across all samples using a Bradford assay (Bio-Rad, Inc). The samples were reduced with 10 mM dithiothreitol at 32°C for 1 hr, followed by alkylation with 40 mM iodoacetamide for 1 hr in the dark. Samples were diluted to 1.8 M Urea with AmBic, then sequencing grade trypsin was added at a 1:25 w/w ratio and digestion proceeded overnight at 32°C. Samples were acidified to 1% TFA, buffer exchanged with Sep Pak C18 (Waters) and lyophilized to dryness. Peptides were resuspended in IAP Buffer (Cell Signaling Technologies) and incubated with a 40 ul aliquot of PTMScan Acetyl-K enrichment kit (11786BK) at 4C overnight. Enriched peptides were eluted with 1% TFA for 10 minutes, dried in a speed-vac, and resuspended in 12 ul 1/2/97 v/v/v TFA/MeCN/water containing

a total of 50 fmol ADH1_YEAST digest (Waters Corporation). LC-MS/MS analysis took place on a nanoAcquity UPLC coupled via electrospray to a LTQ Orbitrap XL mass spectrometer exactly as previously described (20). Database searching for peptide identifications utilized Mascot v2.2 (Matrix Sciences), searching the Uniprot ('reviewed') database (www.uniprot.org) with *homo sapiens* taxonomy, searching the data with 10 ppm precursor and 0.8 Da product ion tolerance, and allowing for variable modifications deamidation (NQ), oxidation (M), and acetylation (K). Quantitative data were processed in Rosetta Elucidator v3.3, allowing relative quantification of all peptides identified in this dataset based on extracted ion chromatograms (peak areas) and accurate-mass and retention time alignment.

Western blotting – HEK-293T and U2OS cells were plated in 10-cm dishes at 75% confluency and transfected with HA-14-3-3ζ expression vector. Cells were trypsinized and plated in up to six 10-cm dishes and allowed to grow for 36 hours. Drug treatments were applied at various concentrations for 6–12 hours as indicated. Cells treated with siRNA knockdown were transfected with HDAC6 siRNA 12 hours after 14-3-3ζ transfection and allowed to grow for 36 hours. Following drug treatment or siRNA transfection, cells were lysed in an ice-cold co-IP buffer (10 mM HEPES pH 7.5, 150 mM KCl, 0.1% NP-40) containing a phosphatase inhibitor cocktail (#88667 Pierce, Rockford, IL, USA), a protease inhibitor cocktail (#88665 Pierce, Rockford, IL, USA), and a pan-HDAC inhibitor cocktail consisting of SAHA (10 μM), Tubacin (40 μM), and Nicotinamide (50 μM; #72340 Sigma, St. Louis, MO, USA). Cell lysates were centrifuged at 21000xg for 10 minutes at 4°C. Supernatant was incubated with 15 μL anti-HA agarose resin (#26181, Pierce, Rockford, IL, USA) for 1.5 hours at 4°C. Following several washes with buffer, resin was boiled with SDS sample buffer (10% SDS, 30% glycerol, 0.7 M beta-mercaptoethanol, 0.15 M Tris, Bromophenol Blue). Samples were loaded and separated on 12% polyacrylamide

gels run along side a Bluestain protein ladder (#P007, GoldBio, St. Louis, MO, USA). Western blots were visualized on LI-COR Odyssey system (Lincoln, NE, USA).

Antibodies – Primary antibodies included: AS160 (#2447S), Atg9 (#13509S), Bad (#9292S), Flag (#8146S), HDAC6 (#7612S), phospho-14-3-3ζ binding motif (#9601S), phospho-AS160 (Thr642, #4288S), and phospho-Bad (Ser112, #9291S) purchased from Cell Signaling Technology (Beverly, MA, USA); 14-3-3ζ (sc-1019), Actin (sc-1616-R), HA (sc-7392), Kinesin (sc-28538), and Liprin-β (sc-22876) purchased from Santa Cruz Biotechnology (Dallas, TX, USA); Polyhistidine provided by Dr. Barry Willardson (Brigham Young University, Provo, Utah, USA). Secondary antibodies purchased from LI-COR (Lincoln, NE, USA) included: Donkey anti rabbit (#926-32213), goat anti mouse (#926-68070), donkey anti mouse (#926-32212), and goat anti rabbit (#926-68071).

Ac-K49 and Ac-K120 antibody purification – Rabbit serum was prepared from animals immunized with an acetylated K49 or K120 peptide sequence conjugated to KLH (Pocono Rabbit Farm and Laboratory, Inc.). Ac-K49 polyclonal antibody was immuno-purified from serum using acetylated K49 peptide as previously described (30). Briefly, biotinylated K49 peptide was bound to streptavidin agarose (#20359, Thermo Scientific, Rockford, IL, USA) and incubated overnight with rabbit serum diluted in buffer (150 mM Tris pH 7.5, 20 mM NaCl) (1:1) in order to deplete serum of non-acetyl specific antibody. After incubation, serum was removed and transferred to acetylated K49 peptide bound to streptavidin resin for overnight incubation. Acetylated K49 bound resin was then washed twice with buffer. Acetyl-specific antibody was eluted off resin using gravity fed elution (100 mM Glycine pH 2.8). Fractions were collected in neutralization buffer (1 M Tris pH 8.5) and tested for antibody titer. Ac-K120 antibody was produced as described above

and purified on a protein-A resin, followed by elution with 100 mM Glycine (pH 2.8) into neutralization buffer (above) to a final pH of 7.5.

In vitro acetylation assay – BL21-DE3 cells were transformed with pGEX-His-14-3-3ζ and grown in LB broth with ampicillin (100 μg/mL). Once O.D. reached 0.6, cells were induced with IPTG (1 mM) and allowed to express for 4 hours. Bacterial cells were pelleted, lysed in buffer (20 mM HEPES, 10 mM KCl, 1.5 mM $MgCl_2$, 1 mM EDTA, 1 mM EGTA, 1 mM DTT, 1 mg/mL lysozyme) containing a protease inhibitor cocktail (#88665 Pierce, Rockford, IL, USA), and treated with DNaseI (2.5 mg/mL). Cell lysate was centrifuged at 21000xg for 10 minutes at 4°C. Supernatant was incubated with 150 μL of nickel resin (H-320-5, GoldBio, St. Louis, MO, USA) for 4 hours at 4°C. After washes with assay buffer (20 mM HEPES, 100 mM NaCl, pH 8.0), a portion of the 14-3-3ζ resin (37.5 μL) was removed for control. Remaining resin (112.5 μL) was incubated with recombinant p300 acetyltransferase enzyme (60 U; purchased from Enzo Life Sciences, BML-SE451-0100) and acetyl-CoA (10 μM) in assay buffer for an hour at 37°C. Following washes, equal portions of the resin were incubated with recombinant HDAC6 enzyme (60 U) alone or HDAC6 enzyme (60 U) with Tubacin (40 μM) for an hour at 37°C. Following additional washes, resin was boiled with SDS sample buffer and separated on a 12% SDS-PAGE gel. Following gel transfer, the membrane was probed with acetyl-K49 antibody.

Gel filtration assay – HEK-293T cells were transfected with HA-14-3-3ζ WT or K49Q mutant expression vector and allowed to express for 48 hours. Cells were then lysed by dounce homogenization using hypotonic lysis buffer (20 mM HEPES, 10 mM KCl, 1.5 mM MgCl2, 1 mM EDTA, 1 mM EGTA, 1 mM DTT) containing a protease inhibitor cocktail (#88665 Pierce, Rockford, IL, USA). 2.5 mg of total protein lysate was loaded onto a superdex 200 10/300 GL gel filtration column running on an AKTA FPLC system (GE healthcare, Pittsburgh, PA, USA). Cell

lysate was fractionated at a flow rate of 500 μL/min using hypotonic lysis buffer. 300 μL elution fractions were collected and separated on a 12% SDS-PAGE gel. Following gel transfer, membranes were probed for HA epitope.

Flow cytometry – HEK-293T cells were plated in 6-cm dishes at a confluency of 75%. Cells were transfected with HA-14-3-3ζ WT or RR mutant expression plasmid. HEK-293T cells were then trypsinized and plated in 6-well plates at 30% initial confluency and allowed to express for 36 hours. Cells were treated with either vehicle or Tubacin (10 μM or 40 μM) for 24 hours. Following treatment, the 6-well plates were prepared for flow cytometry analysis. Briefly, cells were trypsinized and washed twice with cold PBS. Next, cells were resuspended in cold PBS containing 0.2% FBS and 1 μg/ml propidium iodide. Cells were analyzed for cell death using BD Facs Canto system.

RESULTS

14-3-3ζ expression is elevated in receptor-negative breast tumors, and high expression correlates with decreased patient survival—Consistent with the role of 14-3-3ζ in driving multiple oncogenic pathways, previous studies have demonstrated that 14-3-3ζ expression is increased in several cancer types, including breast cancer (11,13,19). To acquire breast cancer subclass-specific information on 14-3-3ζ, we analyzed 14-3-3ζ transcript levels from primary human breast tumors available through The Cancer Genome Atlas (TCGA) database. We found elevated 14-3-3ζ expression levels in the more aggressive basal, HER2-positive, and luminal B subtypes of breast cancer compared to lower expression levels in the typically less aggressive luminal A tumors (Fig. 1A). In addition, we found that breast tumors that lack estrogen and progesterone receptors show higher 14-3-3ζ transcript levels (Fig. 1B). Interestingly, given a previous study showing that 14-

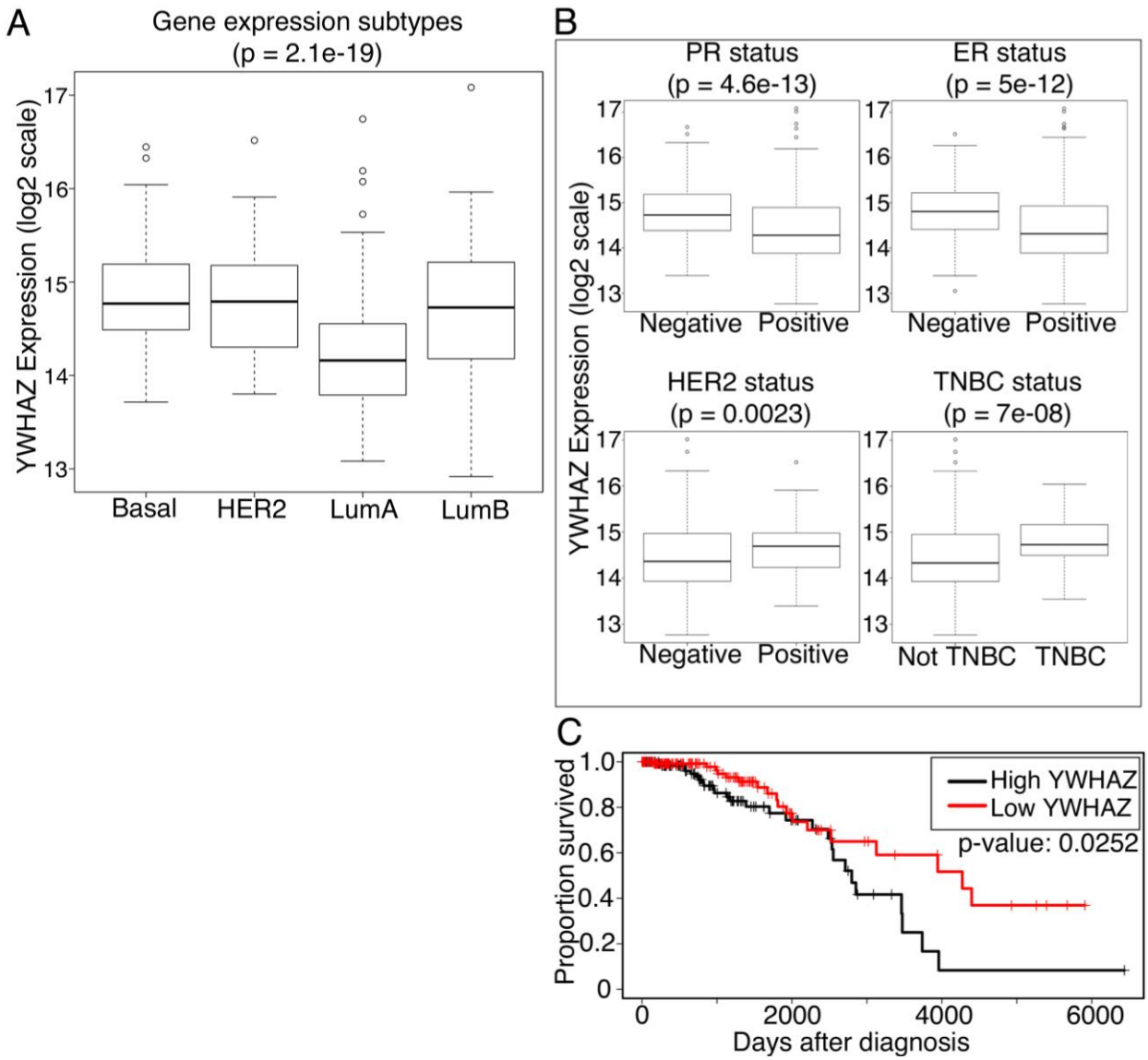

Figure 1. 14-3-3ζ expression is elevated in receptor-negative breast tumors, and high expression correlates with decreased patient survival. (**A**) YWHAZ (14-3-3ζ) expression was analyzed in Basal (n=94), HER2 (n=56), LumA (n=228), and LumB (n=123) breast cancer samples and expressed as Box-and-Whisker plots. *P* value was calculated by comparing all groups with the ANOVA test. (**B**) 14-3-3ζ expression was analyzed in progesterone receptor (PR) positive (n=523), PR negative (n=252), estrogen receptor (ER) positive (n=602), ER negative (n=176), HER2 positive (n=129), HER2 negative (n=429), triple negative breast cancer (TNBC, n=85), and non-TNBC (n=468) data sets. Data are expressed in Box-and-Whisker plots. *P* values were calculated using standard two-sample t-test. (**C**) Kaplan Meier analysis of 14-3-3ζ expression levels correlated with patient survival. Breast cancer patients whose tumors fell within the highest (n=164) and lowest (n=163) quintiles of 14-3-3ζ expression were compared. Statistical significance was calculated using the log-rank test. All data were derived from The Cancer Genome Atlas (TCGA) database.

3-3ζ acts cooperatively with HER2 to drive growth and metastasis in breast cancer (10), we found that 14-3-3ζ expression is higher in HER2-positive tumors (Fig. 1B). Finally, by comparing

patients within the highest and lowest quintiles of 14-3-3ζ expression across all breast cancer subtypes in the TCGA database, we found that high 14-3-3ζ expression is correlated with decreased patient survival (Fig. 1C). Thus, both tumor expression data and our current understanding of 14-3-3ζ-driven pro-growth and survival pathways support the notion of 14-3-3ζ as a therapeutic target to disrupt a hub of oncogenic signaling.

Acetylated lysines within the 14-3-3ζ binding pocket and protein-protein interface—While several groups have worked to develop inhibitors of 14-3-3ζ (reviewed in (21)), these efforts have

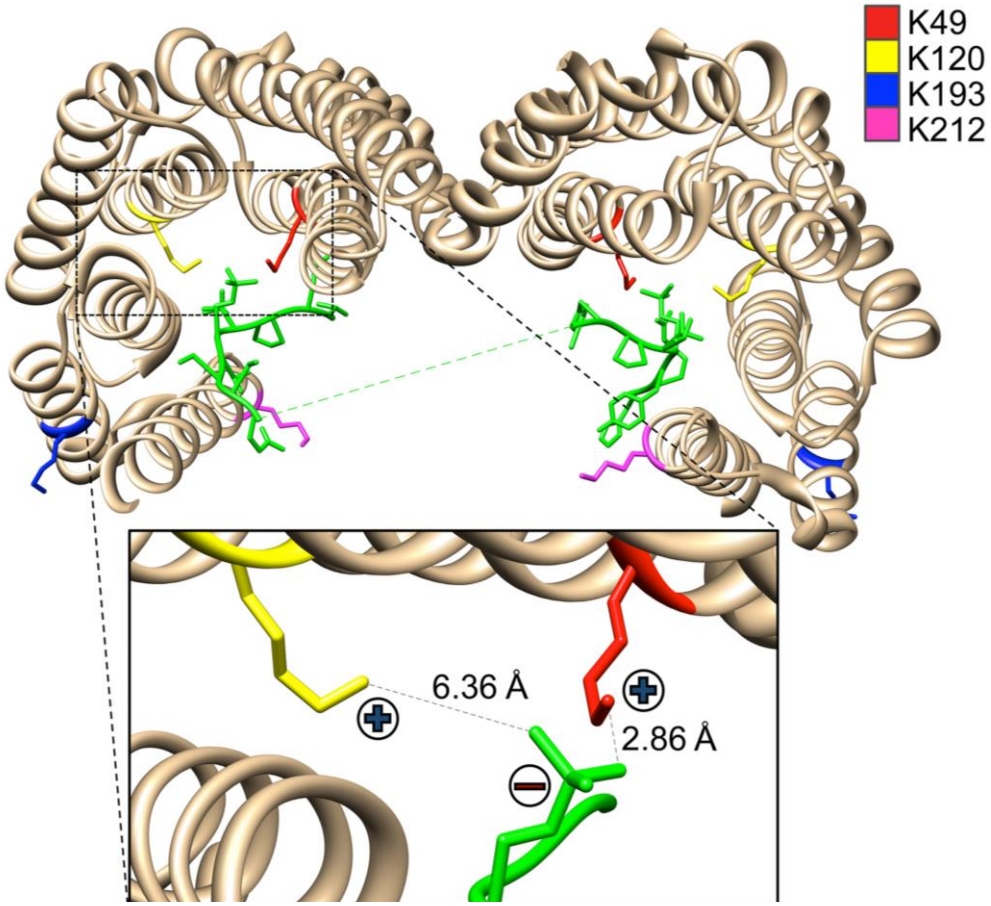

Figure 2. Analysis, we found that several lysines within the 14-3-3ζ binding pocket and protein-protein interface were targets of acetylation. As shown in Figure 2A, which is derived from a published crystal structure of 14-3-3ζ bound to c-Raf (2.2 Å resolution; (32)), two of these lysines, K49 and K120 were previously identified in a large-scale proteomics screen (33) and are posited to interact with the negatively charged Ser/Thr phosphorylation of the binding partner. K49, in particular, is known to be important for 14-3-3ζ interactions (34,35). K193 and K212 are located outside this binding pocket, but within regions of 14-3-3ζ that may interface with the interacting partner.

proven challenging at least partly due to difficulty in developing high-throughput screens for 14-3-3ζ activity (although recent progress has been made in this area (31)). This challenge motivated us to look for other ways to manipulate 14-3-3ζ binding, potentially via 14-3-3ζ regulatory mechanisms. Using immunoprecipitation with acetyl-lysine antibodies followed by LC-MS/MS analysis, we found that several lysines within the 14-3-3ζ binding pocket and protein-protein interface were targets of acetylation. As shown in Figure 2A, which is derived from a published crystal structure of 14-3-3ζ bound to c-Raf (2.2 Å resolution; (32)), two of these lysines, K49 and K120 were previously identified in a large-scale proteomics screen (33) and are posited to interact with the negatively charged Ser/Thr phosphorylation of the binding partner. K49, in particular, is known to be important for 14-3-3ζ interactions (34,35). K193 and K212 are located outside this binding pocket, but within regions of 14-3-3ζ that may interface with the interacting partner.

Acetylation-mimicking mutations abolish 14-3-3ζ interactions—To estimate the impact of each of these acetylations on 14-3-3ζ binding activity, we generated K-to-Q mutations, which mimic the change in charge associated with acetylation. We assessed the binding activity of these mutants by HA-14-3-3ζ overexpression/co-immunoprecipitation (co-IP) and western blotting for several readily detectable 14-3-3ζ interacting proteins, including known interactors such as AS160, Kinesin, and Bad as well as Liprin-β, which we recently identified in an interactomics screen (36) (Fig. 3A). Both the K49Q and K120Q mutations blocked 14-3-3ζ interactions, with K49Q having the most potent inhibitory effect (Fig. 3A). In contrast, we were unable to see any consistent effect with the K193Q and K212Q mutations (Fig. 3A).

To examine the effect of the K49Q mutation on a larger scale, we performed gel filtration chromatography with HEK-293T lysates expressing either HA-tagged WT 14-3-3ζ or the K49Q mutant. Consistent with published reports showing 14-3-3ζ interacting with a wide range of

proteins and protein complexes (37,38), we observed WT 14-3-3ζ across a broad size spectrum ranging from 670 kDa to the 14-3-3ζ dimer near 60 kDa and the 14-3-3ζ monomer at 30 kDa (Fig. 3B). Strikingly, the Q substitution at K49 alone was sufficient to disrupt interactions with high molecular complexes, as this mutant was found shifted into the dimer/monomer range (Fig. 3B).

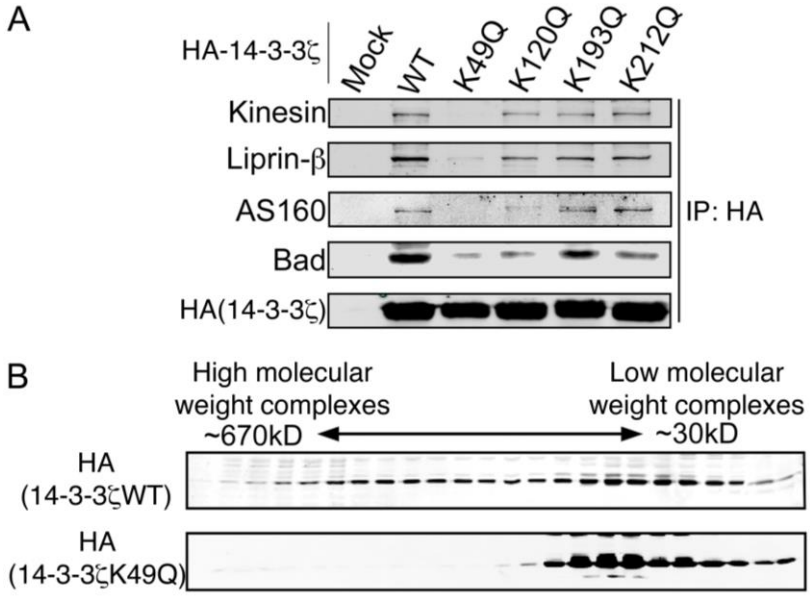

Figure 3. Acetylation-mimicking mutations abolish 14-3-3ζ interactions. (**A**) HEK-293T cells were transfected with WT or mutant forms of HA-tagged 14-3-3ζ plasmid expression vector (K to Q mutants at each acetylated lysine residue). Cell lysates were immunoprecipitated with HA agarose resin and run on 12% SDS-PAGE for immunoblotting for Kinesin, AS160, Liprin-β (36), and Bad. Representative data of at least three replicate experiments. (**B**) HEK-293T cells were transfected with WT or K49Q HA-tagged 14-3-3ζ and subjected to gel filtration. Eluted fractions were collected and run on separate 12% SDS-PAGE for immunoblotting with HA (14-3-3ζ) antibody. Representative data of at least four replicate experiments.

Deacetylation-mimicking mutations rescue the loss of 14-3-3ζ interactions—To determine whether the loss of 14-3-3ζ binding activity caused by the K49Q and K120Q substitutions was due simply to a disruption of the charge as opposed to some other alteration, such as blocking another lysine-targeted post-translational modification, we substituted arginine at K49 and K120 and measured 14-3-3ζ interactions as in Fig. 3A. In addition to the interacting partners mentioned above, we also measured 14-3-3ζ binding to Atg9, which we recently published as a new 14-3-3ζ

binding partner (36). As shown in figure 4A-4B, the K49R/K120R double mutant effectively restores 14-3-3ζ binding activity to at or near WT levels.

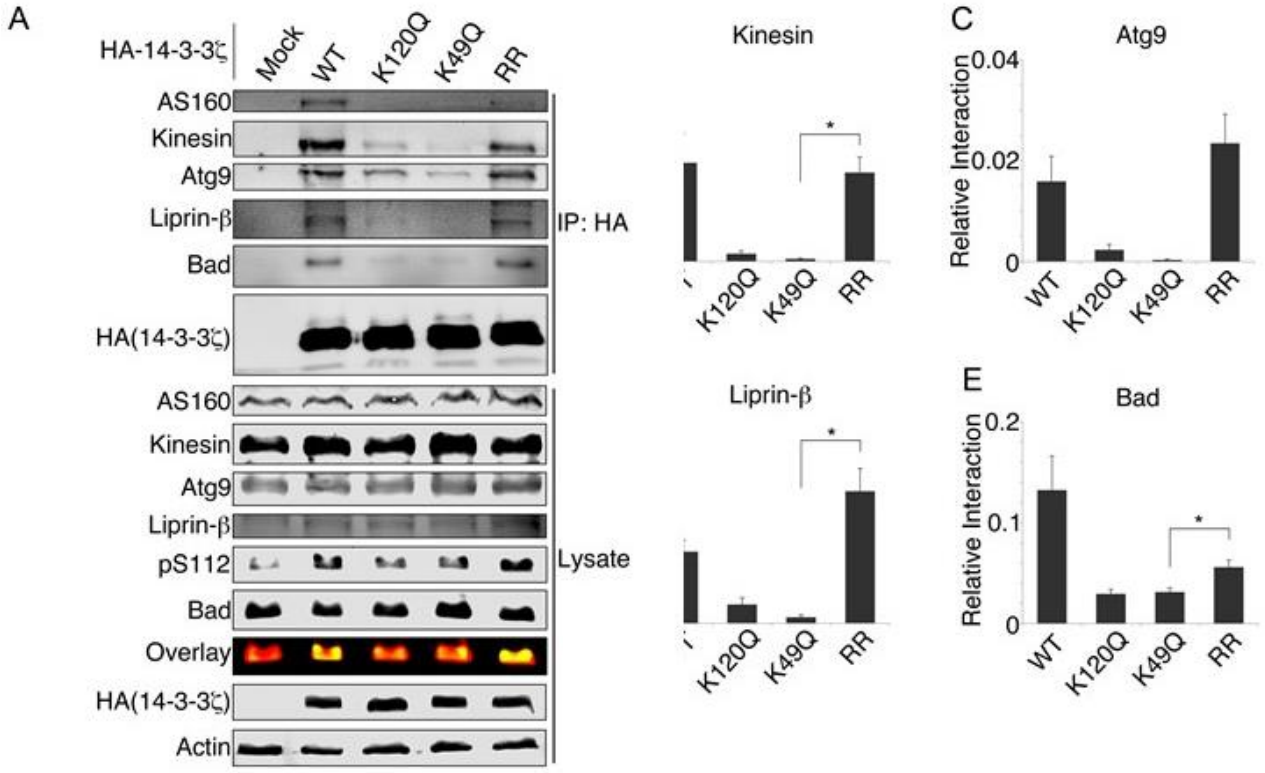

Figure 4. Deacetylation-mimicking mutations rescue the loss of 14-3-3ζ interactions. (**A**) HEK-293T cells were transfected with WT or mutant forms of HA-tagged 14-3-3ζ plasmid expression vector (K to Q mutants at K49 or K120, K to R double mutant at K49 and K120). Cell lysates were immunoprecipitated with HA agarose resin and run on 12% SDS-PAGE for immunoblotting of the binding partners Kinesin, AS160, Liprin-β, Bad, and Atg9 (36). Phosphorylation of 14-3-3ζ binding site of Bad (S112) was compared to total Bad in lysate (overlay). Representative data of at least three replicate experiments. (**B**) Western blot data from seven replicate experiments of panel A were quantified using LI-COR infrared band imaging. Relative interaction values represent the quantified signal of interacting-protein divided by HA signal. *P* values indicated by asterisk were calculated using two-sample T test and are as follows: Kinesin = 0.042; Liprin-β = 0.044; Bad = 0.041

As a measure of 14-3-3ζ binding, we assessed the activation status of Bad by monitoring its phosphorylation at S112. The inhibitory phosphorylation of Bad at S112 and S136 leads to 14-3-3ζ binding (6), which maintains Bad inhibition likely by shielding the phosphorylations from phosphatase activity. We observed an increase in S112 phosphorylation in the presence of WT 14-3-3ζ. Consistent with the interaction data, this increase in S112 phosphorylation was lost in cells expressing the K49Q and K120Q mutants, but recovered by expression of K49R/K120R

(Fig. 4A; see phospho-Bad/Bad overlay). Based on these data and the estimated distance between both K49 and K120 and the phosphate of the binding partner (~3 and ~6 angstroms, respectively; Fig. 2), we posit that acetylation at these sites disrupts a positive-negative electrostatic interaction between the primary amine of lysine and the phosphate that is important for stabilizing the 14-3-3ζ-protein complex (35).

HDAC6 deacetylates 14-3-3ζ at K49 and K120—The strong inhibitory effect of charge disruption at K49 and K120 suggests that modulating the enzymes that govern acetylation at these sites may provide a means to inhibit 14-3-3ζ binding activity. Our attempts to detect acetylation at these sites with pan-acetyl-lysine antibodies yielded inconsistent results. Therefore, we generated site-specific acetyl antibodies to each lysine. Because the Q substitution at K49 had a slightly stronger inhibitory effect on 14-3-3ζ than K120Q, we focused our initial efforts on K49. By treating HEK-293T cells expressing HA-tagged 14-3-3ζ with a panel of deacetylase inhibitors, we found that drugs targeting class I and II HDACs, including Trichostatin A (TSA) and suberanilohydroxamic acid (SAHA), triggered an increase in K49 acetylation (Fig. 5A). In contrast, sirtuin inhibitors showed inconsistent effects on K49 acetylation. EX-527, a Sirt1 and Sirt2 inhibitor, triggered a marginal increase in acetylation, but Salermide, a different Sirt1/2 inhibitor, failed to stimulate such an increase.

Because 14-3-3ζ predominately localizes to the cytoplasm, and HDAC6 is one of the few cytoplasmic HDACs targeted by TSA and SAHA, we reasoned that HDAC6 was a likely culprit. Using the HDAC6-specific inhibitor Tubastatin A (39), we observed a robust increase in K49 acetylation (Fig. 5B). Importantly, mutation of K49 to arginine abolished the Tubastatin A-induced increase in acetylation, indicating the specificity of the antibody (Fig. 5B, last lane). Likewise, Tubacin, a structurally distinct HDAC6 inhibitor (40), also triggered K49 acetylation in the

osteosarcoma cell line U2OS (Fig. 5C). Furthermore, acetylation peaked at 6 hours post-treatment

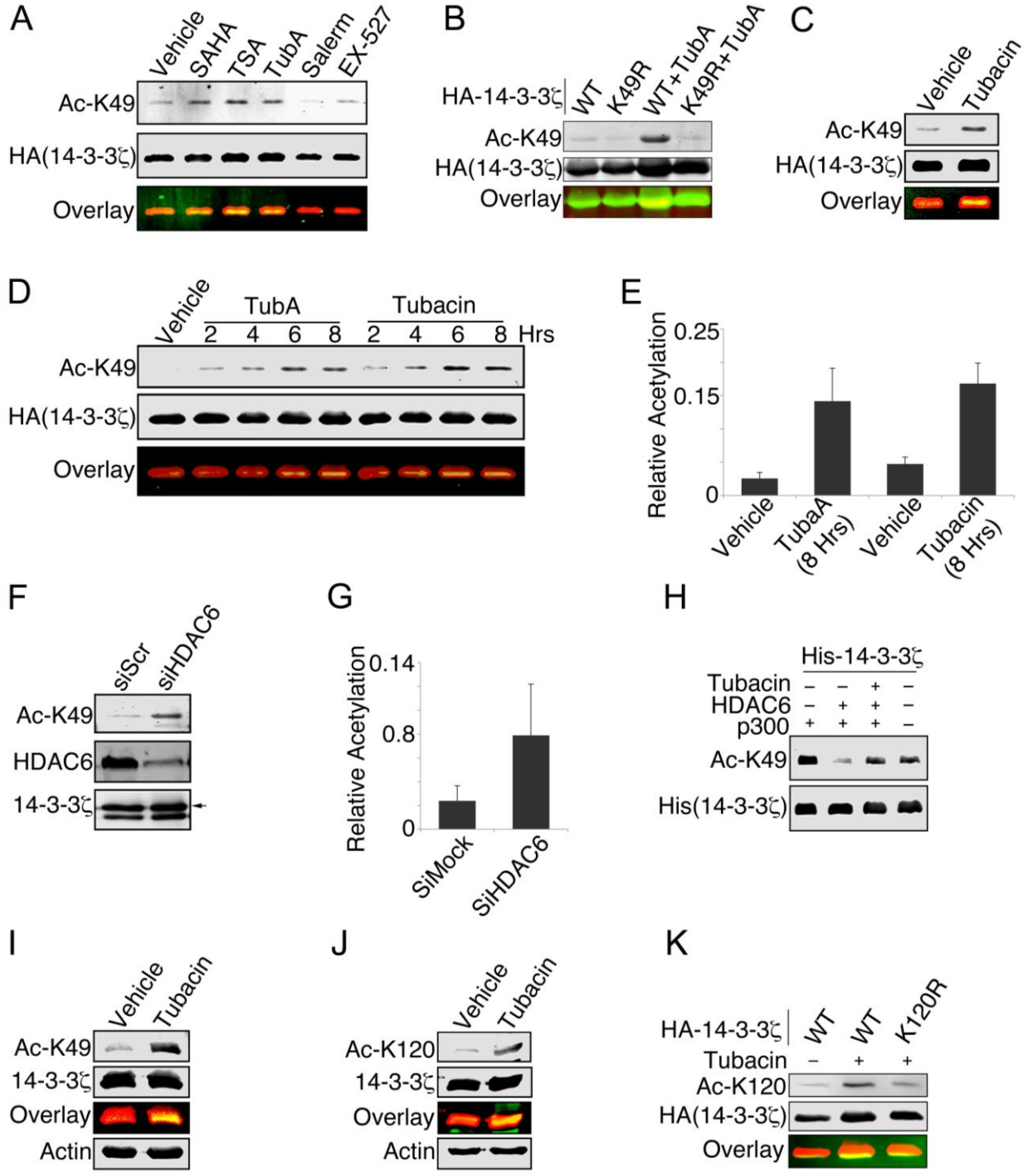

Figure 5. HDAC6 deacetylates 14-3-3ζ at K49 and K120. (**A**) HEK-293T cells were transfected with WT HA-tagged 14-3-3ζ expression vector and treated with various HDAC inhibitor drugs (SAHA 10 μM, Trichostatin A (TSA) 10 μM, Tubastatin A (TubA) 40 μM, Salermide 40 μM, and EX-527 40 μM) or vehicle (DMSO) under normal conditions for 9 hours. Cell lysates were immunoprecipitated with HA resin and run on 12% SDS-PAGE immunoblotting for Ac-K49 (green) and HA (14-3-3ζ, red). Representative data of at least three replicate experiments.

Cont. Figure 5. (**B**) HEK-293T cells overexpressing WT or K49R mutant HA-tagged 14-3-3ζ were treated with Tubastatin A (40 μM) or vehicle for 9 hours followed by HA immunoprecipitation and immunoblot as in Fig. 4A (exception: HA is in green channel, Ac-K49 is in red channel). Representative data of at least four replicate experiments. (**C**) U2OS cells overexpressing WT HA-tagged 14-3-3ζ were treated with Tubacin (30 μM) for 8 hours followed by HA immunoprecipitation and immunoblotting as in Fig. 4A. Representative data of at least three replicate experiments. (**D**) HEK-293T cells overexpressing WT HA-tagged 14-3-3ζ were treated with Tubacin (35 μM) or Tubastatin A (35 μM) in a 2-, 4-, 6-, and 8-hour time course followed by HA immunoprecipitation and immunoblotting as in Fig. 4A. Representative data of at least three replicate experiments. (**E**) 8 hour HDAC6 inhibitor time points from four replicate experiments of panel D were quantified. Relative acetylation signal is Acetyl-K49 signal divided by HA signal. Bands were quantified by LI-COR infrared imaging. (**F**) HEK-293T cells overexpressing WT HA-14-3-3ζ were transfected with HDAC6 siRNA (75 nM) or scrambled siRNA (75 nM). Cell lysates were HA immunoprecipitated and immunoblotted as in Fig. 5A. Representative data of at least three replicate experiments. (**G**) Three replicate experiments from panel F were quantified as in panel E. (**H**) Recombinant His-tagged 14-3-3ζ was expressed in BL21-DE3 *E. coli* and purified on a nickel resin. Resin-bound 14-3-3ζ was incubated with p300 acetyltransferase followed by vehicle, HDAC6 recombinant enzyme, or HDAC6 enzyme and Tubacin (40 μM). 14-3-3ζ was analyzed by 12% SDS-PAGE and immunoblotting with Ac-K49 and His (14-3-3ζ). Representative data of at least three replicate experiments. (**I**) MDA-MB-231 breast cancer cells were treated with Tubacin (30 μM) or vehicle for 8 hours. Endogenous 14-3-3ζ was analyzed by resolving cell lysate (40 μg) using 12% SDS-PAGE and immunoblotting with Ac-K120 (green), 14-3-3ζ (red), and Actin. Representative data of at least three replicate experiments. (**J**) MDA-MB-231 breast cancer cells were treated as in Fig. 4G. Endogenous 14-3-3ζ was analyzed as in Fig. 4G. Representative data of at least three replicate experiments. (**K**) HEK-293T cells overexpressing WT or K120R mutant HA-tagged 14-3-3ζ were treated with Tubacin (40 μM) or vehicle for 9 hours followed by HA immunoprecipitation and immunoblotting with Ac-K120 (green) and HA (red). Representative data of at least three replicate experiments.

for both drugs (Fig. 5D). Figure 5E shows the quantified data of the HDAC6 inhibitor-induced increase in K49 acetylation from four experiments. To rule out potential off-target effects of drug treatment, we confirmed that siRNA against HDAC6 induced K49 acetylation (Fig. 5F and G) and recombinant HDAC6 was capable of deacetylating K49 *in vitro* (Fig. 5H).

Next, we asked whether we could detect acetylation of endogenous 14-3-3ζ. Consistent with our previous results, treatment of the triple negative breast cancer line MDA-MB-231 with Tubacin triggered acetylation of endogenous 14-3-3ζ at K49 (Fig. 5I). Given the proximity of K49 and K120 in the 3-dimensional structure of 14-3-3ζ, we suspected that both lysines were substrates of HDAC6. Indeed, HDAC6 inhibition resulted in acetylation of K120, as detected on endogenous 14-3-3ζ in MDA-MB-231 cells (Fig. 5J) and immunoprecipitated HA-tagged 14-3-3ζ from HEK-293T cells (Fig. 5K). As in Fig. 4B, the K120R mutant served as a specificity control for the acetyl-

K120 antibody (Fig. 5K, last lane). Taken together, these data suggest that HDAC6 deacetylates K49 and K120 and thereby may regulate 14-3-3ζ binding activity.

Inhibition of HDAC6 triggers a loss of 14-3-3ζ interactions and an increase in cell death, both of which are rescued by the K49R/K120R double mutant—Our data suggest a model in which high HDAC6 activity promotes 14-3-3ζ binding activity by maintaining K49 and K120 in their deacetylated states. Conversely, as suggested by data in Figure 5, HDAC6 inhibition allows a progressive build up of acetylation (presumably catalyzed by an unidentified acetyl-transferase) at these residues. To test whether this increase in acetylation induces a loss of 14-3-3ζ binding activity, we chose to focus on the 14-3-3ζ-interacting proteins AS160 and Bad. AS160 is a Rab-GTPase activating protein involved in GLUT4 translocation to cell membranes. Once on the membrane, GLUT4 serves as a major receptor for glucose uptake in breast, multiple myeloma and other cancers (3-5). Phosphorylation of AS160 at T642 triggers the binding of 14-3-3 proteins (ζ and other isoforms), which leads to AS160 activation and GLUT4 translocation (2,41). Bad is a pro-apoptotic BH3-only protein that transduces an apoptotic signal to mitochondria in response to various chemotherapeutics (6-9). Phoshorylation of Bad at S112, as well as S136, leads to 14-3-3 binding and Bad inhibition (6). Both of these proteins can be readily detected in overexpression/co-IP experiments with 14-3-3ζ.

Using HEK-293T cells and FLAG-AS160 immunoprecipitation, we found that HDAC6 inhibition decreases AS160-14-3-3ζ binding (Fig. 6A, lanes 2–3). Importantly, the loss of AS160-14-3-3ζ interaction was rescued by the K49R/K120R 14-3-3ζ mutant (Fig. 6A, lanes 4–5), suggesting that acetylation is the key event triggering disruption of the complex. We also performed the converse immunoprecipitation experiment with HA-14-3-3ζ and Bad. Consistent with data in Figure 6A, inhibition of HDAC6 triggers a decrease in the 14-3-3ζ-Bad interaction,

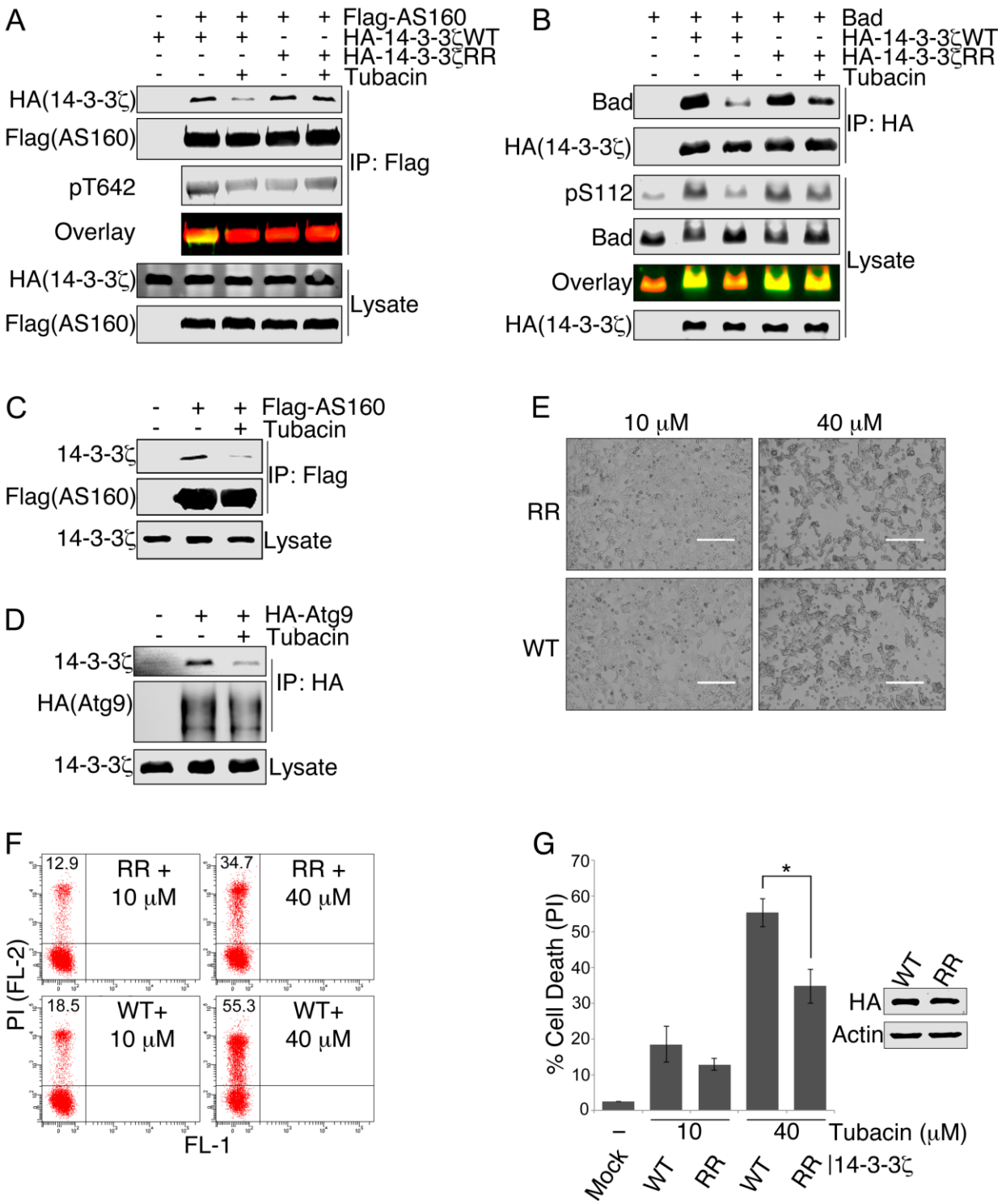

Figure 6. Inhibition of HDAC6 triggers a loss of 14-3-3ζ interactions and an increase in cell death, both of which are rescued by the K49R/K120R double mutant. (**A**) HEK-293T cells were co-transfected with WT Flag-tagged AS160 expression plasmid along with either WT HA-tagged 14-3-3ζ, or K49R/K120R (RR) double mutant expression plasmid, followed by treatment with Tubacin (30 μM) or vehicle for 6 hours. Cell lysates were immunoprecipitated using Flag agarose and run on 12% SDS-PAGE

Cont. Figure 6. for immunoblotting with HA (14-3-3ζ), pT642 (phosphothreonine642), and Flag (AS160). Representative data of at least three replicate experiments. (**B**) HEK-293T cells were co-transfected with Bad expression plasmid along with either WT HA-tagged 14-3-3ζ, or K49R/K120R (RR) double mutant expression plasmid, followed by treatment with Tubacin (30 μM) or vehicle for 9 hours. Cell lysates were immunoprecipitated using HA agarose and run on 12% SDS-PAGE for immunoblotting with Bad and HA (14-3-3ζ). Cell lysate was immunoblotted with pS112 (phosphoserine112). Representative data of at least three replicate experiments. (**C**) HEK-293T cells were transfected with WT Flag-tagged AS160 expression plasmid or mock followed by treatment with Tubacin (40 μM) or vehicle for 6 hours. Cell lysates were immunoprecipitated using Flag agarose and run on 12% SDS-PAGE for immunoblotting with 14-3-3ζ and Flag (AS160). Representative data of at least four replicate experiments. (**D**) HEK-293T cells were transfected with WT HA-tagged Atg9 expression plasmid or mock followed by treatment with Tubacin (40 μM) or vehicle for 6 hours. Cell lysates were immunoprecipitated using HA agarose and run on 12% SDS-PAGE for immunobloting with 14-3-3ζ and HA (Atg9). Representative data of at least four replicate experiments. (**E**) HEK-293T cells overexpressing either WT 14-3-3ζ, K49R/K120R (RR) double mutant 14-3-3ζ, or mock transfection were treated with Tubacin (10 μM, 40 μM) or vehicle for 48 hours. Cell death was measured by PI staining and flow cytometry. Data presented as light microscope pictures (scale bar = 250 μm), or (**F**) Flow cytometry dot plots, or (**G**) Bar graph (mean±SEM, n=3, p-value=0.029). *P* value was calculated using two-sample T test. Inset is a immunoblot comparing expression of WT or RR mutant 14-3-3ζ. Cell lysates were analyzed via 12% SDS-PAGE and immunoblot. Membrane was probed for HA (14-3-3ζ) and actin.

which is rescued by the K49R/K120R mutant (Fig. 6B). Furthermore, as shown in Figures 6C and 6D, HDAC6 inhibition effectively dissociates endogenous 14-3-3ζ from overexpressed interacting partners AS160 and Atg9.

A critical function of 14-3-3 proteins is their ability to protect phosphorylations from removal by phosphatases. For example, 14-3-3 binding to an inhibitory phosphorylation on Cdc25 protects it from protein phosphatase-1 activity, thereby preventing Cdc25 activation and entry into M phase (42). Thus, we reasoned that forcing disruption of 14-3-3ζ via K49/K120 acetylation should lead to dephosphorylation of the interacting partner. Indeed, phosphorylation of AS160 at T642 and Bad at S112 tracked with 14-3-3ζ binding, showing decreased phosphorylation in cells treated with HDAC6 inhibitor, and more importantly, a recovery of phosphorylation (albeit only a marginal recovery with AS160) in the presence of the K49R/K120R mutant despite HDAC6 inhibition (Fig. 6A and 6B, see overlay images).

HDAC6 inhibition enhances stress-induced cell death, and HDAC6 inhibitors are currently being evaluated as potential therapeutics in cancer (28,43). HDAC6 has only a few bonafide substrates, including its best characterized substrate tubulin, as well as HSP90, cortactin and MSH2 (43,44). To test the role of 14-3-3ζ acetylation in the toxicity of HDAC6 inhibition, we analyzed the cytoprotective effect of both WT 14-3-3ζ and the K49R/K120R mutant (compared to mock controls) against HDAC6 inhibitor-induced cell death. Although the non-acetylatable mutant was unable to completely suppress cell death (supporting the involvement of other HDAC6 substrates), it showed a significantly enhanced cytoprotective effect compared to WT 14-3-3ζ (Figs. 6E–G). These data suggest that inhibitory acetylation of 14-3-3ζ contributes to HDAC6 inhibitor-induced cell death. Based on these results, we posit that the exploitation of 14-3-3ζ pathways with combination therapies may enhance the anti-tumor effect of HDAC6 inhibitors.

DISCUSSION

As a phospho-binding protein, 14-3-3ζ has been implicated in numerous pro-growth pathways, and both *in vitro* and *in vivo* data point toward its function as an oncogene (reviewed in (13)). We show here a new and potentially exploitable mechanism of 14-3-3ζ control by HDAC6. Specifically, we demonstrate that 14-3-3ζ can be suppressed by HDAC6 inhibition and consequent acetylation of K49 and K120, which sit within the 14-3-3ζ binding pocket. These data raise several questions addressed below.

The position of K49 and K120 within the 14-3-3ζ binding pocket raises the question of how acetylation occurs if the residues are buried between 14-3-3ζ and the interacting partner. Since 14-3-3ζ exists in equilibrium between bound and unbound states, we favor the idea that the unbound “free” pool of 14-3-3ζ is subjected to deacetylation/acetylation. This idea is supported by

our unpublished *in vitro* experiments in which we could only acetylate recombinant 14-3-3ζ (using the p300 catalytic domain as in Fig. 5H) when in the unbound form. Conversely, incubation of 14-3-3ζ with a purified interacting partner prevented acetylation, suggesting that lysines within the binding pocket may be inaccessible to KAT activity when 14-3-3ζ is in a bound complex. In this model, HDAC6 inhibition and acetylation of 14-3-3ζ simply shift the bound-to-unbound equilibrium, increasing the pool of unbound 14-3-3ζ (Fig. 7).

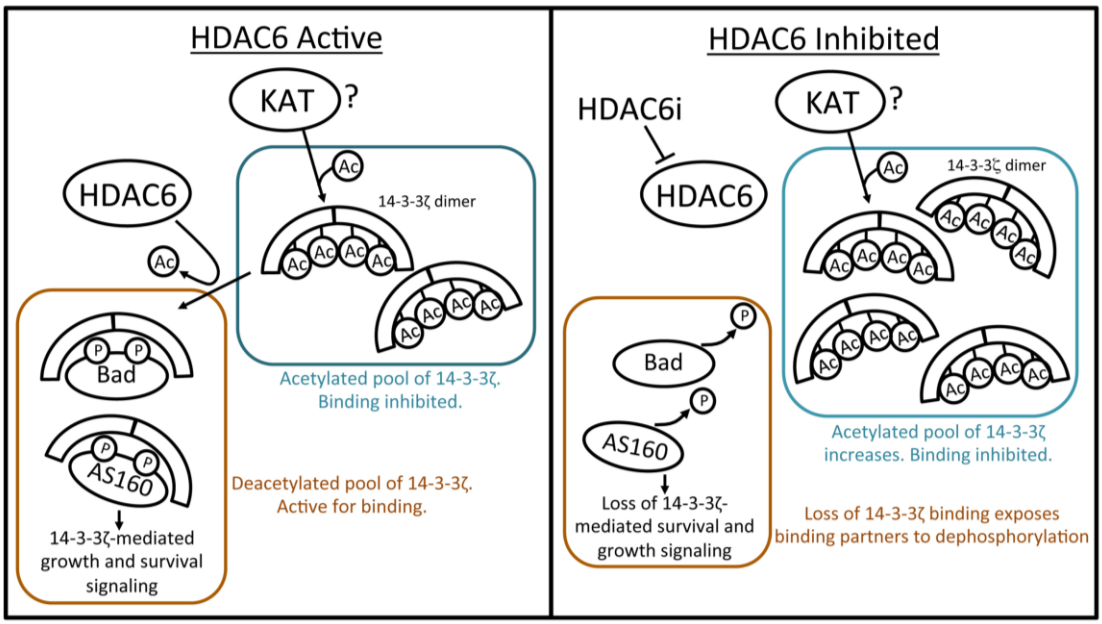

Figure 7. HDAC6 maintains 14-3-3ζ (shown as a dimer) binding activity by deacetylating K49 and K120 within the 14-3-3ζ binding pocket. Inhibition of HDAC6 leads to 14-3-3ζ acetylation and loss of 14-3-3ζ binding activity. Acetylation-induced dissociation of 14-3-3ζ interactions (e.g., with Bad and AS160) results in a loss of pro-growth signaling. The KAT that acetylates K49 and K120 is unknown.

Another question raised by these data is whether HDAC6 inhibition and consequent acetylation of K49 result in the global loss of 14-3-3ζ interacting partners. We suspect that this is not the case given the vast array of 14-3-3ζ interacting partners (37) and the only partially overlapping localization of HDAC6 and 14-3-3ζ. Thus, it seems more likely that the various pools of 14-3-3ζ (e.g., nuclear, cytosolic, membrane-associated, etc.) may be regulated by different KATs and KDACs. Notably, in a previous study using an unbiased biotin-switch proteomics

approach in Xenopus eggs, we identified 14-3-3ζ as one of several putative substrates of Sirt1 (14). However, as shown in Figure 5A, we observed a very minor increase in K49 acetylation with EX-527 (a Sirt1 inhibitor) when compared to HDAC6 inhibition, which had the most robust effect in human cell lines. In future studies, it will be important to identify the subset of 14-3-3ζ interacting partners affected by HDAC6 inhibition as well as other KDACs (and KATs) that might regulate acetylation at K49 in different cellular compartments.

One compartment in which HDAC6 and 14-3-3ζ are likely to be intertwined is in the cytoskeletal and microtubule network. A key pro-survival function of HDAC6 is to recruit misfolded proteins to microtubule-associated dynein motor complexes for transport to aggresomes, which alleviates the toxic accumulation of misfolded proteins in cells (45-48). Interestingly, 14-3-3 has recently been implicated in aggresome formation (49). Specifically, 14-3-3 proteins have been shown to interact with and promote the association of the dynein motor complex with the Bcl-2-associate athanogene 3 (BAG3), a co-chaperone protein that helps target misfolded proteins to aggresomes (49). Thus, the deacetylation of 14-3-3ζ and consequent maintenance of its binding activity may be part of the mechanism of HDAC6-mediated aggresome formation. Our observation that acetylation-refractory mutants of 14-3-3ζ protect cells from HDAC6 inhibitors is consistent with this idea (Fig. 6E–G). HDAC6 and 14-3-3ζ also associate with tau (50,51), a microtubule-associated protein involved in neurodegeneration. 14-3-3ζ binding to tau promotes tau hyperphosphorylation and is implicated in the formation of toxic tau lesions in Alzheimer's disease brains (50,52). In future studies, it will be important to determine the role that HDAC6 plays in regulating these and other functions of 14-3-3ζ.

The strong inhibitory effect of acetylation on 14-3-3ζ binding raises the question of why and when would these acetylations occur physiologically. Under high growth conditions, HDAC6

activity appears to stay consistently high, which would lead to a low stoichiometry of acetylation. In turn, active 14-3-3ζ would reinforce pro-growth signaling. Indeed, our LC-MS/MS analysis of total 14-3-3ζ immunoprecipitated from cells indicates a low baseline level of acetylation under normal growth conditions (Andersen, unpublished). A study by Xiaohong Zhang and colleagues found that HDAC6 is phosphorylated by ERK, which increases HDAC6 activity and promotes cell motility (53). Thus we speculate that the acetylation status of 14-3-3ζ is dictated by pro-growth signaling. For example, growth factor withdrawal may lead to increased 14-3-3ζ acetylation as a result of lower ERK-mediated HDAC6 activity. This seems likely given that 14-3-3ζ promotes numerous cell growth pathways and therefore would need to be shut off during quiescence.

In summary, our data highlight a novel role for HDAC6 in the regulation of 14-3-3ζ. Going forward, it will be critical to determine the full impact of HDAC6 inhibition on the vast network of 14-3-3ζ interactions, and whether other 14-3-3 family members are similarly regulated, as this may illuminate novel combination strategies to enhance the efficacy of HDAC6 inhibitors.

REFERENCES

1. Yang, X., Cao, W., Zhang, L., Zhang, W., Zhang, X., and Lin, H. Targeting 14-3-3zeta in cancer therapy. *Cancer gene therapy.* **2012**, 19, 153-159
2. Chen, S., Synowsky, S., Tinti, M., and MacKintosh, C. The capture of phosphoproteins by 14-3-3 proteins mediates actions of insulin. *Trends in endocrinology and metabolism: TEM.* **2011**, 22, 429-436
3. Cheng, J. C., McBrayer, S. K., Coarfa, C., Dalva-Aydemir, S., Gunaratne, P. H., Carpten, J. D., Keats, J. K., Rosen, S. T., and Shanmugam, M. Expression and phosphorylation of the AS160_v2 splice variant supports GLUT4 activation and the Warburg effect in multiple myeloma. *Cancer & metabolism.* **2013**, 1, 14
4. McBrayer, S. K., Cheng, J. C., Singhal, S., Krett, N. L., Rosen, S. T., and Shanmugam, M. Multiple myeloma exhibits novel dependence on GLUT4, GLUT8, and GLUT11: implications for glucose transporter-directed therapy. *Blood.* **2012**, 119, 4686-4697
5. Garrido, P., Osorio, F. G., Moran, J., Cabello, E., Alonso, A., Freije, J. M., and Gonzalez, C. Loss of GLUT4 induces metabolic reprogramming and impairs viability of breast cancer cells. *Journal of cellular physiology.* **2015**, 230, 191-198
6. Danial, N. N. BAD: undertaker by night, candyman by day. *Oncogene.* **2008**, 27 Suppl 1, S53-70
7. Danial, N. N., Gramm, C. F., Scorrano, L., Zhang, C. Y., Krauss, S., Ranger, A. M., Datta, S. R., Greenberg, M. E., Licklider, L. J., Lowell, B. B., Gygi, S. P., and Korsmeyer, S. J. BAD and glucokinase reside in a mitochondrial complex that integrates glycolysis and apoptosis. *Nature.* **2003**, 424, 952-956
8. Datta, S. R., Katsov, A., Hu, L., Petros, A., Fesik, S. W., Yaffe, M. B., and Greenberg, M. E. 14-3-3 proteins and survival kinases cooperate to inactivate BAD by BH3 domain phosphorylation. *Molecular cell.* **2000**, 6, 41-51
9. Zha, J., Harada, H., Yang, E., Jockel, J., and Korsmeyer, S. J. Serine phosphorylation of death agonist BAD in response to survival factor results in binding to 14-3-3 not BCL-X(L). *Cell.* **1996**, 87, 619-628
10. Lu, J., Guo, H., Treekitkarnmongkol, W., Li, P., Zhang, J., Shi, B., Ling, C., Zhou, X., Chen, T., Chiao, P. J., Feng, X., Seewaldt, V. L., Muller, W. J., Sahin, A., Hung, M. C., and Yu, D. 14-3-3zeta Cooperates with ErbB2 to promote ductal carcinoma in situ progression to invasive breast cancer by inducing epithelial-mesenchymal transition. *Cancer cell.* **2009**, 16, 195-207
11. Neal, C. L., Yao, J., Yang, W., Zhou, X., Nguyen, N. T., Lu, J., Danes, C. G., Guo, H., Lan, K. H., Ensor, J., Hittelman, W., Hung, M. C., and Yu, D. 14-3-3zeta overexpression defines high risk for breast cancer recurrence and promotes cancer cell survival. *Cancer research.* **2009**, 69, 3425-3432
12. Li, Z., Zhao, J., Du, Y., Park, H. R., Sun, S. Y., Bernal-Mizrachi, L., Aitken, A., Khuri, F. R., and Fu, H. Down-regulation of 14-3-3zeta suppresses anchorage-independent growth of lung cancer cells through anoikis activation. *Proceedings of the National Academy of Sciences of the United States of America.* **2008**, 105, 162-167
13. Neal, C. L., and Yu, D. 14-3-3zeta as a prognostic marker and therapeutic target for cancer. *Expert opinion on therapeutic targets.* **2010**, 14, 1343-1354
14. Andersen, J. L., Thompson, J. W., Lindblom, K. R., Johnson, E. S., Yang, C. S., Lilley, L. R., Freel, C. D., Moseley, M. A., and Kornbluth, S. A biotin switch-based proteomics

approach identifies 14-3-3zeta as a target of Sirt1 in the metabolic regulation of caspase-2. *Molecular cell.* **2011**, 43, 834-842
15. Nutt, L. K., Buchakjian, M. R., Gan, E., Darbandi, R., Yoon, S. Y., Wu, J. Q., Miyamoto, Y. J., Gibbons, J. A., Andersen, J. L., Freel, C. D., Tang, W., He, C., Kurokawa, M., Wang, Y., Margolis, S. S., Fissore, R. A., and Kornbluth, S. Metabolic control of oocyte apoptosis mediated by 14-3-3zeta-regulated dephosphorylation of caspase-2. *Dev Cell.* **2009**, 16, 856-866
16. Brunet, A., Bonni, A., Zigmond, M. J., Lin, M. Z., Juo, P., Hu, L. S., Anderson, M. J., Arden, K. C., Blenis, J., and Greenberg, M. E. Akt promotes cell survival by phosphorylating and inhibiting a Forkhead transcription factor. *Cell.* **1999**, 96, 857-868
17. Maxwell, S. A., Li, Z., Jaye, D., Ballard, S., Ferrell, J., and Fu, H. 14-3-3zeta mediates resistance of diffuse large B cell lymphoma to an anthracycline-based chemotherapeutic regimen. *The Journal of biological chemistry.* **2009**, 284, 22379-22389
18. Lin, M., Morrison, C. D., Jones, S., Mohamed, N., Bacher, J., and Plass, C. Copy number gain and oncogenic activity of YWHAZ/14-3-3zeta in head and neck squamous cell carcinoma. *International journal of cancer. Journal international du cancer.* **2009**, 125, 603-611
19. Bergamaschi, A., Frasor, J., Borgen, K., Stanculescu, A., Johnson, P., Rowland, K., Wiley, E. L., and Katzenellenbogen, B. S. 14-3-3zeta as a predictor of early time to recurrence and distant metastasis in hormone receptor-positive and -negative breast cancers. *Breast cancer research and treatment.* **2013**, 137, 689-696
20. Matta, A., Siu, K. W., and Ralhan, R. 14-3-3 zeta as novel molecular target for cancer therapy. *Expert opinion on therapeutic targets.* **2012**, 16, 515-523
21. Zhao, J., Meyerkord, C. L., Du, Y., Khuri, F. R., and Fu, H. 14-3-3 proteins as potential therapeutic targets. *Seminars in cell & developmental biology.* **2011**, 22, 705-712
22. Margolis, S. S., Perry, J. A., Forester, C. M., Nutt, L. K., Guo, Y., Jardim, M. J., Thomenius, M. J., Freel, C. D., Darbandi, R., Ahn, J. H., Arroyo, J. D., Wang, X. F., Shenolikar, S., Nairn, A. C., Dunphy, W. G., Hahn, W. C., Virshup, D. M., and Kornbluth, S. Role for the PP2A/B56delta phosphatase in regulating 14-3-3 release from Cdc25 to control mitosis. *Cell.* **2006**, 127, 759-773
23. DeYoung, M. P., Horak, P., Sofer, A., Sgroi, D., and Ellisen, L. W. Hypoxia regulates TSC1/2-mTOR signaling and tumor suppression through REDD1-mediated 14-3-3 shuttling. *Genes & development.* **2008**, 22, 239-251
24. Powell, D. W., Rane, M. J., Chen, Q., Singh, S., and McLeish, K. R. Identification of 14-3-3zeta as a protein kinase B/Akt substrate. *The Journal of biological chemistry.* **2002**, 277, 21639-21642
25. Woodcock, J. M., Murphy, J., Stomski, F. C., Berndt, M. C., and Lopez, A. F. The dimeric versus monomeric status of 14-3-3zeta is controlled by phosphorylation of Ser58 at the dimer interface. *The Journal of biological chemistry.* **2003**, 278, 36323-36327
26. Aldana-Masangkay, G. I., and Sakamoto, K. M. The role of HDAC6 in cancer. *Journal of biomedicine & biotechnology.* **2011**, 2011, 875824
27. Namdar, M., Perez, G., Ngo, L., and Marks, P. A. Selective inhibition of histone deacetylase 6 (HDAC6) induces DNA damage and sensitizes transformed cells to anticancer agents. *Proceedings of the National Academy of Sciences of the United States of America.* **2010**, 107, 20003-20008

28. Santo, L., Hideshima, T., Kung, A. L., Tseng, J. C., Tamang, D., Yang, M., Jarpe, M., van Duzer, J. H., Mazitschek, R., Ogier, W. C., Cirstea, D., Rodig, S., Eda, H., Scullen, T., Canavese, M., Bradner, J., Anderson, K. C., Jones, S. S., and Raje, N. Preclinical activity, pharmacodynamic, and pharmacokinetic properties of a selective HDAC6 inhibitor, ACY-1215, in combination with bortezomib in multiple myeloma. *Blood.* **2012**, 119, 2579-2589
29. Yang, P. H., Zhang, L., Zhang, Y. J., Zhang, J., and Xu, W. F. HDAC6: Physiological function and its selective inhibitors for cancer treatment. *Drug discoveries & therapeutics.* **2013**, 7, 233-242
30. Goto, H., and Inagaki, M. Production of a site- and phosphorylation state-specific antibody. *Nature protocols.* **2007**, 2, 2574-2581
31. Du, Y., Fu, R. W., Lou, B., Zhao, J., Qui, M., Khuri, F. R., and Fu, H. A time-resolved fluorescence resonance energy transfer assay for high-throughput screening of 14-3-3 protein-protein interaction inhibitors. *Assay and drug development technologies.* **2013**, 11, 367-381
32. Molzan, M., Kasper, S., Roglin, L., Skwarczynska, M., Sassa, T., Inoue, T., Breitenbuecher, F., Ohkanda, J., Kato, N., Schuler, M., and Ottmann, C. Stabilization of physical RAF/14-3-3 interaction by cotylenin A as treatment strategy for RAS mutant cancers. *ACS chemical biology.* **2013**, 8, 1869-1875
33. Choudhary, C., Kumar, C., Gnad, F., Nielsen, M. L., Rehman, M., Walther, T. C., Olsen, J. V., and Mann, M. Lysine acetylation targets protein complexes and co-regulates major cellular functions. *Science.* **2009**, 325, 834-840
34. Fu, H., Subramanian, R. R., and Masters, S. C. 14-3-3 proteins: structure, function, and regulation. *Annual review of pharmacology and toxicology* **2000**, 40, 617-647
35. Gardino, A. K., Smerdon, S. J., and Yaffe, M. B. Structural determinants of 14-3-3 binding specificities and regulation of subcellular localization of 14-3-3-ligand complexes: a comparison of the X-ray crystal structures of all human 14-3-3 isoforms. *Seminars in cancer biology.* **2006**, 16, 173-182
36. Weerasekara, V. K., Panek, D. J., Broadbent, D. G., Mortenson, J. B., Mathis, A. D., Logan, G. N., Prince, J. T., Thomson, D. M., Thompson, J. W., and Andersen, J. L. Metabolic stress-induced rearrangement of the 14-3-3zeta interactome promotes autophagy via a ULK1- and AMPK-regulated 14-3-3zeta interaction with phosphorylated Atg9A. *Molecular and cellular biology.* **2014**,
37. Ge, F., Li, W. L., Bi, L. J., Tao, S. C., Zhang, Z. P., and Zhang, X. E. Identification of novel 14-3-3zeta interacting proteins by quantitative immunoprecipitation combined with knockdown (QUICK). *Journal of proteome research.* **2010**, 9, 5848-5858
38. Pozuelo-Rubio, M. Proteomic and biochemical analysis of 14-3-3-binding proteins during C2-ceramide-induced apoptosis. *The FEBS journal.* **2010**, 277, 3321-3342
39. Butler, K. V., Kalin, J., Brochier, C., Vistoli, G., Langley, B., and Kozikowski, A. P. Rational design and simple chemistry yield a superior, neuroprotective HDAC6 inhibitor, tubastatin A. *Journal of the American Chemical Society.* **2010**, 132, 10842-10846
40. Haggarty, S. J., Koeller, K. M., Wong, J. C., Grozinger, C. M., and Schreiber, S. L. Domain-selective small-molecule inhibitor of histone deacetylase 6 (HDAC6)-mediated tubulin deacetylation. *Proceedings of the National Academy of Sciences of the United States of America.* **2003**, 100, 4389-4394
41. Stockli, J., Davey, J. R., Hohnen-Behrens, C., Xu, A., James, D. E., and Ramm, G. Regulation of glucose transporter 4 translocation by the Rab guanosine triphosphatase-

activating protein AS160/TBC1D4: role of phosphorylation and membrane association. *Mol Endocrinol.* **2008**, 22, 2703-2715

42. Margolis, S. S., Walsh, S., Weiser, D. C., Yoshida, M., Shenolikar, S., and Kornbluth, S. PP1 control of M phase entry exerted through 14-3-3-regulated Cdc25 dephosphorylation. *The EMBO journal.* **2003**, 22, 5734-5745
43. Yan, J. Interplay between HDAC6 and its interacting partners: essential roles in the aggresome-autophagy pathway and neurodegenerative diseases. *DNA and cell biology.* **2014**, 33, 567-580
44. Zhang, M., Xiang, S., Joo, H. Y., Wang, L., Williams, K. A., Liu, W., Hu, C., Tong, D., Haakenson, J., Wang, C., Zhang, S., Pavlovicz, R. E., Jones, A., Schmidt, K. H., Tang, J., Dong, H., Shan, B., Fang, B., Radhakrishnan, R., Glazer, P. M., Matthias, P., Koomen, J., Seto, E., Bepler, G., Nicosia, S. V., Chen, J., Li, C., Gu, L., Li, G. M., Bai, W., Wang, H., and Zhang, X. HDAC6 deacetylates and ubiquitinates MSH2 to maintain proper levels of MutSalpha. *Molecular cell.* **2014** 55, 31-46
45. Kawaguchi, Y., Kovacs, J. J., McLaurin, A., Vance, J. M., Ito, A., and Yao, T. P. The deacetylase HDAC6 regulates aggresome formation and cell viability in response to misfolded protein stress. *Cell.* **2003**, 115, 727-738
46. Lee, J. Y., Nagano, Y., Taylor, J. P., Lim, K. L., and Yao, T. P. Disease-causing mutations in parkin impair mitochondrial ubiquitination, aggregation, and HDAC6-dependent mitophagy. *The Journal of cell biology.* **2010**, 189, 671-679
47. Wang, L., Xiang, S., Williams, K. A., Dong, H., Bai, W., Nicosia, S. V., Khochbin, S., Bepler, G., and Zhang, X. Depletion of HDAC6 enhances cisplatin-induced DNA damage and apoptosis in non-small cell lung cancer cells. *PloS one.* **2012**, 7, e44265
48. Zhang, X., Yuan, Z., Zhang, Y., Yong, S., Salas-Burgos, A., Koomen, J., Olashaw, N., Parsons, J. T., Yang, X. J., Dent, S. R., Yao, T. P., Lane, W. S., and Seto, E. HDAC6 modulates cell motility by altering the acetylation level of cortactin. *Molecular cell.* **2007**, 27, 197-213
49. Xu, Z., Graham, K., Foote, M., Liang, F., Rizkallah, R., Hurt, M., Wang, Y., Wu, Y., and Zhou, Y. 14-3-3 protein targets misfolded chaperone-associated proteins to aggresomes. *Journal of cell science.* **2013**, 126, 4173-4186
50. Hashiguchi, M., Sobue, K., and Paudel, H. K. 14-3-3zeta is an effector of tau protein phosphorylation. *The Journal of biological chemistry.* **2000**, 275, 25247-25254
51. Ding, H., Dolan, P. J., and Johnson, G. V. Histone deacetylase 6 interacts with the microtubule-associated protein tau. *Journal of neurochemistry.* **2008**, 106, 2119-2130
52. Qureshi, H. Y., Li, T., MacDonald, R., Cho, C. M., Leclerc, N., and Paudel, H. K. Interaction of 14-3-3zeta with microtubule-associated protein tau within Alzheimer's disease neurofibrillary tangles. *Biochemistry* **2013**, 52, 6445-6455
53. Williams, K. A., Zhang, M., Xiang, S., Hu, C., Wu, J. Y., Zhang, S., Ryan, M., Cox, A. D., Der, C. J., Fang, B., Koomen, J., Haura, E., Bepler, G., Nicosia, S. V., Matthias, P., Wang, C., Bai, W., and Zhang, X. Extracellular signal-regulated kinase (ERK) phosphorylates histone deacetylase 6 (HDAC6) at serine 1035 to stimulate cell migration. *The Journal of biological chemistry* **2013**, 288, 33156-33170

CHAPTER 4: DISCUSSION

Lysine acetylation has become an important topic in cytosolic cellular regulation. The utility of specific and non-specific inhibition of proper acetylation regulation in cancer cells is being aggressively explored in clinical trials. We wanted to investigate how breast cancer cells changed their cytosolic acetylation under the physiologically relevant metabolic stress of hypoxia. We hoped this would give us some insight into which acetylation(s) may be important for a tumor cell's ability to cope with a lethal metabolic environment. Given the ability of tumor cells to survive hypoxia, we also sought to determine whether widespread deregulation of acetylation via small molecule inhibitors would promote cell death in hypoxia. This would lend more weight of evidence to the use of such chemotherapies against tumor cells.

Our finding indicate that breast tumor cells, which are very adept at hypoxia survival, are able to tightly regulate their acetylation(s) from normoxia to hypoxia. The fact that hypoxia didn't cause as big of a change to acetylation status for the tumor cells could be due to tumor cells being pre-adapted to survival under such conditions. These cells may have a PTM preset for metabolic stress and are therefore much more likely to survive the rapid/transient hypoxia that they are exposed to. If this is the case, tumor cells would be especially susceptible to acetylation deregulation via small molecule inhibitors. Our findings would lend support to this hypothesis. Using a general HDAC inhibitor we were able to show tumor cells being sensitized to hypoxia-induced cell death. The specific lysine residues which are more critical to the survival of a tumor cell must be investigated further. If we can identify important lysine residues on pro-survival protein targets, we can then find how they are regulated thus giving us the ability to target more critical acetylation pathways in tumor cells.

Using general HDAC inhibitors which disrupt cellular acetylation has been a useful approach. Using a specific HDAC inhibitor could have a similar sensitizing impact on tumor cells without causing undesired off-target effects. This of course would require investigation into which acetylation regulating enzymes are more critical to tumor cell survival. To investigate this we used a siRNA knockdown approach to determine which protein targets were more necessary to hypoxia survival. Our date show several targets which cause a decreased ability to survive hypoxia when depleted from cells. HDAC6, being one of those targets, has been used to develop specific inhibitors for chemotherapy drug trials. Indeed knockdown of HDAC6 alone showed an increase in cell death in hypoxia resistant tumor cells, demonstrating the usefulness of HDAC6 as a drug target.

While understanding that HDAC6 is critical to tumor cell survival is necessary to designing specific drug treatments, It is also very useful to understand which targets of HDAC6 would help account for its pro-survival activity. To date very few substrates of HDAC6 have been found. If we can find pro-survival targets of HDAC6 then there is the possibility of multi-pathway drug designing, using one drug to inhibit HDAC6 and another to inhibit another pathway which could compound the effectiveness of the both drugs. Fortunately we identified a substrate of HDAC6 which is critical to the survival of tumor cells. We identified lysine residues of 14-3-3ζ which were acetylated, some of which were critical to the function of the protein. We then used a screening approach to identify the HDAC that regulated these critical acetylation events. Using various techniques and approaches, we were able to determine that HDAC6 regulates 14-3-3ζ via deacetylation of lysine 49 and 120. This information sheds light on the various pathways which HDAC6 may be regulating through 14-3-3ζ. Further work must be done to identify which 14-3-3ζ pathways are disrupted through HDAC6 inhibition. The pathways that we identified in our study

are a good starting point for further investigation. If the disruption of 14-3-3ζ interaction with AS160 or Bad can be recapitulated *in vivo* we may be able to combine HDAC6 inhibition with a pro-apoptotic Bad mimetic or a chemotherapy which targets glucose utilization. These are just two of the many 14-3-3ζ mediated pathways which have potential for combinatorial drug therapy.

Another question is raised by our work is which acetyltransferase is responsible for the addition of acetyl groups to 14-3-3ζ? This question must be addressed to gain a full understanding of how 14-3-3ζ is regulated via acetylation. Will we see a change in acetylation status of 14-3-3ζ if we inhibit acetyltransferase activity? We may not see a change in acetylation status if it is controlled primarily through HDAC6 activity. In other words, if the acetylation is held at a very low level by HDAC6 we may not see any difference after actyeltransferase inhibition. This could mean that some acetylation events may necessarily be held in tight control to prevent cell death. These questions must be answered not only for how 14-3-3ζ is regulated, but how acetylation events regulate other critical proteins in the tumor cell.

The field of non-histone acetylation has become important to the understanding of how cells are regulated. Much more must be done to further our understanding of how tumor cells use acetylation to become tumorigenic and survive normally lethal environments. The tools of mass spectrometry and immune-detection have come a long way, though more needs to be done to be able to ask critical question in the field of acetylation.